INVESTIGATION OF THE MOLECULAR PATHWAYS INVOLVED IN
INTESTINAL EPITHELIAL DIFFERENTIATION

A THESIS SUBMITTED TO
THE GRADUATE SCHOOL OF NATURAL AND APPLIED SCIENCES
OF
MIDDLE EAST TECHNICAL UNIVERSITY

BY

ASLI SADE MEMİŞOĞLU

IN PARTIAL FULFILLMENT OF THE REQUIREMENTS
FOR
THE DEGREE OF DOCTOR OF PHILOSOPHY
IN
BIOLOGY

JANUARY 2014

Approval of the thesis:

INVESTIGATION OF THE MOLECULAR PATHWAYS INVOLVED IN
INTESTINAL EPITHELIAL DIFFERENTIATION

submitted by **ASLI SADE MEMİŞOĞLU** in partial fulfillment of the requirements
for the degree of **Doctor of Philosophy in Biology Department, Middle East
Technical University** by,

Prof. Dr. Canan Özgen   _____
Dean, Graduate School of **Natural and Applied Sciences**

Prof. Dr. Gülay Özcengiz   _____
Head of Department, **Biology**

Assoc. Prof. Dr. Sreeparna Banerjee   _____
Supervisor, **Biology Dept., METU**

Examining Committee Members:

Assoc. Prof. Dr. Mesut Muyan   _____
Biology Dept., METU

Assoc. Prof. Dr. Sreeparna Banerjee   _____
Biology Dept., METU

Assoc. Prof. Dr. Elif Erson Bensan   _____
Biology Dept., METU

Assoc. Prof. Dr. Çetin Kocaefe   _____
Medical Biology Dept., Hacettepe University

Assoc. Prof. Dr. Ali Osmay Güre   _____
Molecular Biology Dept., Bilkent University

Date: 24/01/14

I hereby declare that all information in this document has been obtained and presented in accordance with academic rules and ethical conduct. I also declare that, as required by these rules and conduct, I have fully cited and referenced all material and results that are not original to this work.

Name, Last name: Aslı Sade Memişoğlu

Signature   :

ABSTRACT

INVESTIGATION OF THE MOLECULAR PATHWAYS INVOLVED IN INTESTINAL EPITHELIAL DIFFERENTIATION

Sade Memişoğlu, Aslı

Ph.D., Department of Biology

Supervisor: Assoc. Prof. Dr. Sreeparna Banerjee

January 2014, 95 pages

The molecular mechanisms of balanced and continuous generation of intestinal epithelial cells, is poorly understood and disruption of this balance may result in neoplastic transformation and malignant growth. Differentiation is regulated by numerous signals, which in turn regulate signaling pathways directing activation or inactivation of certain transcription factors. Perturbations like changes in Ca^{2+} levels, glucose or amino acid starvation result in an ER stress response, which is also implicated in the differentiation process. In addition, ER stress and autophagy pathways may function together under certain circumstances. The transcription factor C/EBPβ is of particular importance, as it is implicated in differentiation, ER stress and autophagy.

In the current study, using two models of colorectal cancer cell lines, HT-29 and Caco-2 that can undergo differentiation, ER stress response was shown to be activated during the process of differentiation. Ca^{2+} flux into the cytoplasm was found to be the mediator of ER stress response in Caco-2 cells. Interestingly, ER stress caused induction of autophagy during differentiation in both cell lines.

Moreover, C/EBPβ-3, the short isoform of C/EBPβ, was found to be one of the key players in the activation of autophagy.

ER stress induced autophagy and involvement of C/EBPβ-3 in these processes was for the first time evidenced in the differentiation of Caco-2 and HT-29 cell lines. These results suggest new regulatory mechanisms that may be of significance in the process of intestinal epithelial differentiation.

Key words: differentiation, colorectal cancer, C/EBPβ, ER stress, autophagy.

ÖZ

BAĞIRSAK EPİTEL FARKLILAŞMASINDA YER ALAN MOLEKÜLER YOLAKLARIN ARAŞTIRILMASI

Sade Memişoğlu, Aslı

Doktora, Biyoloji Bölümü

Tez Yöneticisi: Doç. Dr. Sreeparna Banerjee

Ocak 2014, 95 sayfa

Bağırsak epitel hücrelerinin dengeli ve sürekli üretimi ile ilgili moleküler mekanizmalar iyi anlaşılmış değildir ve bu dengenin bozulması neoplastik transformasyona ve maliknant büyümeye yol açabilir. Karmaşık bir süreç olan farklılaşma çeşitli hücre dışı ve içi sinyaller, sinyal yolakları ve bunların aktive veya inhibe ettiği transkripsiyon faktörleri tarafından düzenlenmektedir. Ca^{2+} seviyelerindeki değişimler, glikoz veya amino asit yoksunluğu gibi düzensizlikler farklılaşma sürecinde de belirtilen ER stres yanıtına yol açar. Ayrıca, ER stres ve otofaji yolakları belirli koşullarda birlikte etki gösterebilirler. Farklılaşma, ER stres ve otofaji süreçlerinde belirtilen bir transkripsiyon faktörü olan C/EBPβ özellikle önem kazanmaktadır.

Bu çalışmada, farklılaşma modeli olan iki kolorektal hücre hattı HT-29 ve Caco-2 kullanılarak, bağırsak epitel farklılaşmasında ER stres yanıtının aktif duruma geldiği gösterilmiştir. Ayrıca, Caco-2 farklılaşmasında sitoplazmaya Ca^{2+} boşalımının ER strese sebep olduğu belirlenmiştir. İlginçtir ki, her iki hücre hattında da ER stres

otofajiye yol açmıştır. Bunlara ek olarak ER stres kaynaklı otofajiye C/EBPβ küçük izoformu C/EBPβ-3 aracılık ettiği anlaşılmıştır.

Caco-2 ve HT-29 farklılaşmasında ER stress kaynaklı otofajinin varlığı ve C/EBPβ-3'ün bu süreçteki rolü ilk defa olarak ortaya konmuştur. Bu bulgular, bağırsak epitel farklılaşmasının regülasyonunda yeni mekanizmalar öne sürmektedir.

Anahtar kelimeler: Farklılaşma, kolorektal kanser, C/EBPβ, ER stress, otofaji.

To My Family

ACKNOWLEDGEMENTS

I express my sincere gratitude to my supervisor Dr. Sreeparna Banerjee for her valuable guidance, encouragement and understanding throughout the research.

I am thankful to Dr. Elif Erson Bensan, Dr. Mesut Muyan, Dr Çetin Kocaefe, Dr. Ali Osmay Güre, Dr. Ebru Erbay, and Dr. Özlen Konu for their invaluable discussions, guidance and sharing resources throughout the whole process.

I am also thankful to Dr. Devrim Gözüaçık and Dr. Tamotsu Yoshimori for sharing antibodies and plasmids.

I would like to thank my lab mates for their sincere friendship, support and comments throughout the study.

I am grateful to Seda Tunçay Çağatay for being the best companion during all these years.

My special gratitudes go to my parents and my sister for their encouragement, support and patience which can never be remunerated.

I am grateful to my husband Kerem Memişoğlu for his years of patience and support from long distances.

TABLE OF CONTENTS

APPENDICES

LIST OF TABLES

TABLES

LIST OF FIGURES

CHAPTER 1

INTRODUCTION

1.1 Intestinal differentiation

The epithelium of the gastrointestinal (GI) tract is under continuous renewal and plays a pivotal role in maintaining intestinal homeostasis via a highly controlled differentiation program along the crypt-villus axis (Barbara et al., 2003). The process is characterized by the proliferation of stem cells residing near the base of the intestinal crypts and subsequent differentiation, as cells migrate from the crypt to the villus, into one of the four major cell types. The enterocytes (absorptive cells) are the most abundant intestinal epithelial cells. These cells are characterized by the presence of brush border membranes associated with tight junctions on their apical surface and expression of brush border hydrolases like sucrase isomaltase and alkaline phosphatase. Goblet cells constitute 5% of the intestinal epithelium and are responsible for mucus production. Enteroendocrine cells constitute a small proportion of the intestine and function in GI motility by producing certain hormones. Paneth cells are mostly related to antimicrobial defense. The localization of intestinal epithelial cells differs according to their differentiation status along the crypt-villus axis; undifferentiated cells at the bottom and more differentiated ones at the top, except for Paneth cells which reside at the bottom of the crypts (Fig. 1.1) (Barbara et al., 2003).

The process of terminal differentiation is associated with an irreversible withdrawal from the cell cycle and the expression of various tissue-specific genes. The molecular mechanism of balanced and continuous generation of intestinal epithelial cells is a poorly understood phenomenon and disruption of this balance may result in

neoplastic transformation and malignant growth (Ilantzis et al., 2002; Pignatelli et al., 1992; Solanas et al., 2008). The cells constituting epithelial tumors show a dedifferentiated phenotype in which the expression of epithelial specific genes like E-cadherin are lost and they acquire the ability to proliferate and metastasize (Johnson, 1999; Solanas et al., 2008).
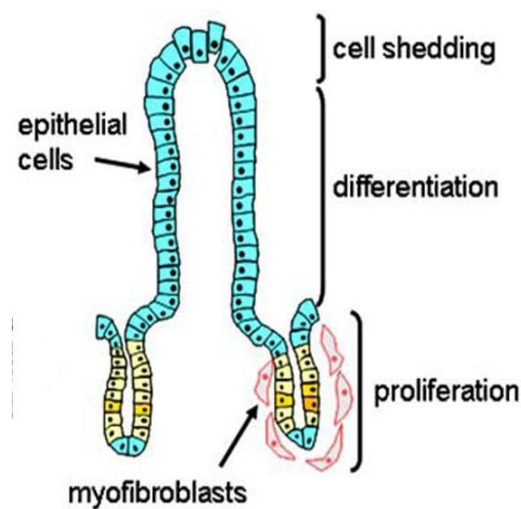
Fig. 1.1 The crypt-villus axis of the intestinal epithelium (Simon-Assman et al., 2007).

1.2   Models of intestinal differentiation

Understanding the mechanisms underlying the differentiation-dedifferentiation processes has become the focus of a growing number of researchers because of the importance of these events in normal intestinal homeostasis, development and disease. However, the induction of apoptosis in the primary intestinal epithelial cultures soon after dissection from the tissue is a major drawback in differentiation

2

studies (Burgess, 1998). The colon carcinoma cell lines Caco-2 and HT-29, established by J. Fogh (Fogh et al., 1977), have gained attention because of their ability to differentiate in certain culture conditions showing mature enterocyte like characteristics (Pinto et al., 1982; Pinto et al., 1983). These cells, when differentiated, are very similar to intestinal epithelial cells in terms of morphology and expression of brush border hydrolases. The expression of small intestine brush border hydrolases by differentiated colonic cells is noteworthy since normal colon cells do not express these enzymes. It was later realized that the same hydrolases are actually present in the fetal colon (Lacroix et al., 1984). However, one also has to keep in mind that these cells are malignant cells harboring mutations in their genomes, which constitutes a major drawback of the models. Despite the limitations, these cell lines became well established *in vitro* models of differentiation of the intestinal epithelium and have been extensively used worldwide (Simon-Assman et al., 2007).

1.2.1 Caco-2 cell line

Caco-2 is a relatively well-differentiated colorectal cancer cell line that can undergo enterocytic differentiation spontaneously, when grown to confluency under standard culture conditions (Simon-Assman, 2007). These cells form polarized monolayers associated with tight junctions and present well-developed microvilli starting from day 7 with a gradual increase up to day 20 after confluency (Fig. 1.2).
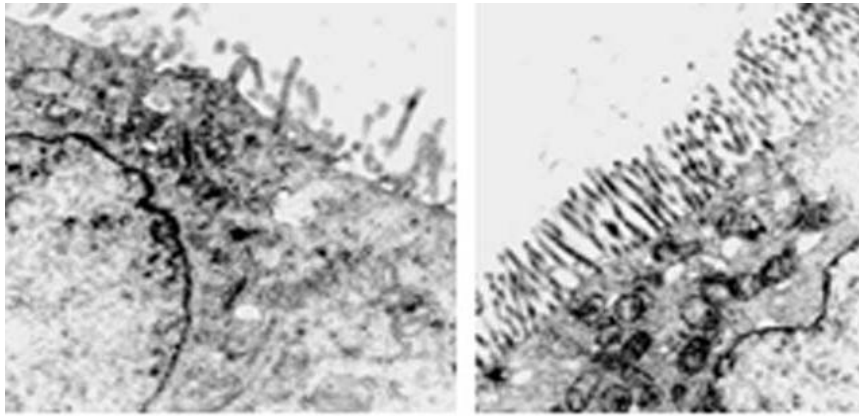
Fig. 1.2 Electron micrographs comparing microvilli of undifferentiated (left) and differentiated (right) Caco-2 cells (Simon-Assman et al., 2007).

In addition to the morphological changes, Caco-2 cells also show functional characteristics of mature enterocytes, such as the expression of brush border hydrolases (alkaline phosphatase, sucrase isomaltase and dipeptidyl peptidase IV) and formation of domes, indicative of transepithelial ionic transport (Rousset, 1986; Simon-Assman et al., 2007).

Caco-2 cell line has been used as a differentiation model for nearly thirty years and is sensitive to culturing conditions and passage number. One important aspect of differentiation of Caco-2 cells is the heterogeneity of the parental line, which is reflected in the passages used in different laboratories (Sambuy et al., 2005). As the cells are grown and passaged in differing conditions, the cells with certain characteristics over the others are selected and start to dominate the population. Attempts to standardize the culture conditions have been made and some more homogenous sub-clones, some of which do not show all the characteristics of the parental cell line, have also been generated in the recent years (Behrens and Kissel, 2003; Sambuy et al., 2005).

1.2.2 HT-29 cell line

HT-29 has been shown to have high rates of glucose consumption and under standard culture conditions are not differentiated. This cell line is considered to be pluripotent as the cells have the ability to differentiate into distinct types of epithelial cells under specific culture conditions or differentiation inducers. When HT-29 cells are grown in the absence of glucose; either replaced by galactose (Pinto et al., 1982), inosine or uridine (Wice et al., 1985) or no hexose at all (Zweibaum et al., 1985), these cells show a reversible enterocytic differentiation, similar to Caco-2 cells, forming monolayers with tight junctions and expressing brush border hydrolases, although the activities are not as high as in Caco-2 cells or normal intestine. In the absence of serum, on the other hand, 50% of the cells show characteristics of goblet cells with the presence of mucins (Zweibaum et al., 1982).

Caco-2 and HT-29 cell lines are currently being used as models of the intestinal epithelium for a wide range of studies on the regulation of cell polarity, cell signaling, regulation of ion transport and the biological pathways in the development and treatment of cancer (Rousset, 1986; Simon-Assman, 2007).

1.3   Molecular pathways involved in intestinal epithelial differentiation

The complex process of differentiation is regulated by numerous intra- and extracellular signals generated by growth factors, cell-cell and cell-matrix interactions which in turn regulate signaling pathways directing activation or inactivation of certain transcription factors, chromosome remodeling complexes and their targets. The differentiated cells of the normal intestinal epithelium and also the two differentiation models of colorectal cancer cells form cell-cell adhesions to perform barrier function.

The specific molecular mechanisms regulating intestinal epithelial differentiation are poorly understood. One of the primary changes that terminally differentiated cells undergo is their exit from the cell cycle, leading to an eventual event of programmed cell death at the mucosal surface. Mariadason *et al.* (Mariadason et al., 2000) have

shown that Caco-2 cells undergo cell cycle arrest at G_1. p21 was proposed to be partially responsible for the cell cycle arrest (Evers et al., 1996) together with suppression of Cdk2 and Cdk4 (Ding et al., 1998). Regulation of the cell cycle transcription factor E2F through its interaction with Rb-related protein p300 and phosphorylation may also be another mechanism regulating Caco-2 differentiation (Ding et al., 2000). Additionally, the process of cellular differentiation is largely dependent on intracellular Ca^{2+} levels. It is known that dietary Ca^{2+} stops colon cell proliferation and tumorigenesis and induces differentiation (Whitfield, 2009). Intracellular Ca^{2+} pools of the cell have been shown to exert significant control over cell growth and progression through the cell cycle and depletion of Ca^{2+} stores leads to G_0 like arrest (Ghosh et al., 1991; Short et al., 1993). Ca^{2+} mobilization from the ER stores were observed during the differentiation of both gastric cancer cells (Papp et al., 2004) and colonic crypts (Lindqvist et al., 1998). This mobilization was proposed to have resulted from an increase in the levels of sarco/endoplasmic reticulum calcium transport ATPase3 (SERCA3). It has been stated that since SERCA3 has lower affinity for Ca^{2+}, an increase in the levels of SERCA3 results in higher cytoplasmic and diminished ER calcium levels (Lytton et al., 1992). In accordance with this, loss of SERCA3 expression was found to be an early event during colon carcinogenesis (Brouland et al., 2005).

1.4   Endoplasmic reticulum (ER) stress

The most important function of the ER is proper folding of secretory and membrane proteins. Additionally it stores calcium for localized release and lipogenic reactions take place in the ER lumen. Recently developed mouse models revealed that the ER also helps maintain cellular homeostasis, control energy metabolism, inflammation and differentiation (Rutkowski and Hegde, 2010). Perturbations like changes in the Ca^{2+} levels, glucose or amino acid starvation, viral infections, interfere with the ER chaperone machinery, misfolded proteins accumulate and result in ER stress (Marciniak and Ron, 2006). This activates an evolutionarily conserved series of events termed the unfolded protein response (UPR).

6

In mammals there are three sensors of ER stress; activated transcription factor 6 (ATF6), inositol-requiring enzyme 1α (IRE1α) and PKR like ER kinase (PERK) (Walter and Ron, 2011), which are kept inactive by the ER chaperone B cell immunoglobulin protein (BiP). Misfolded or unfolded proteins bind this chaperone inhibiting its interaction with the sensor proteins. These ER resident transmembrane proteins regulate the three branches of the UPR, all of which result in the activation of bZIP transcription factors and consequent expression of UPR associated genes (Fig. 1.3). ATF6 translocates to the Golgi upon stimuli where it is processed to give rise to the active basic leucine zipper (bZIP) transcription factor. This is followed by the translocation of ATF6 into the nucleus and transcription of several genes together with XBP1. IRE1α is activated by oligomerization and *trans*-autophosphorylation leading to activation of its RNase domain. The activated enzyme cleaves a 26bp region from an intron of X-box binding protein 1 (XBP1) mRNA leading to a more stable XBP1s mRNA. Translation of the spliced XBP1 (sXBP1) produces a highly active transcription factor, which works in concert with the bZIP transcription factors of the UPR and transactivates target genes involved in the response. Activation of PERK is similar to that of IRE1α in which its dimerization and *trans*-autophosphorylation causes the phosphorylation of its target protein eukaryotic translation initiation factor 2α (eIF2α). The phosphorylated form of eIF2α is unable to bind GTP, which results in a global inhibition of translation and the protein load of ER. Interestingly this low rate translation leads to an increase in the translation of bZIP transcription factors like activating transcription factor 4 (ATF4) (Hetz et al., 2013; Walter and Ron, 2011). The mechanism underlying this selective translation involves the differential usage of upstream open reading frames (uORFs). These uORFs are out of frame with the main protein coding region and therefore act as translational repressors of the mRNA. When the levels of eIF2α-GTP fall during UPR, the repressor sequences are not translated and the translational machinery finds time to scan the mRNA until the actual start codon (Donnelly et al., 2013). ATF4 is involved in the the expression of chaperone proteins, lipid metabolism and UPR related genes.
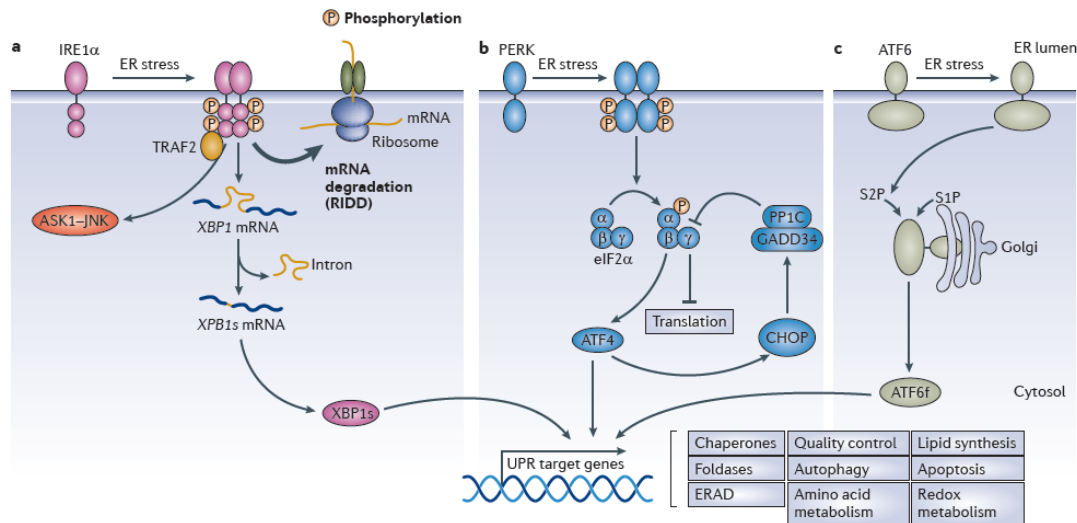
Fig. 1.3 The three main pathways involved in ER stress (Hetz et al., 2013).

Although UPR is an adaptive mechanism of cells to stress conditions, it also activates apoptotic pathways under prolonged ER stress. The mechanism of the switch from adaptive to apoptotic pathways is still not well known. This dual role of UPR is also implicated in development and progression of cancer. Tumor cells are subjected to high metabolic needs due to rapid proliferation, and stress due to limiting nutrient and oxygen supply. UPR therefore may help cancer cells adapt these conditions. On the other hand death activating consequences of UPR may also be important in eliminating transforming cells from the population.

1.4.1   ER stress and differentiation

ER stress is a part of normal development program of certain tissues or organ systems (Zhang et al., 2007). For example, a difference in the ER capacity may lead to a phentypical change, such as differentiation. In such a case XBP-1 was found to be necessary for the differentiation of plasma cells (Reimold et al., 2001). ER stress

8

is also activated in epidermal keratinocyte differentiation (Sugiura et al., 2009), mouse neuronal differentiation of ESCs (Cho et al., 2009) and retinoic acid induced human ESC differentiation (Liu et al., 2012). Organs with predominantly secretory cells such as the intestinal epithelium very frequently require the UPR for homeostasis. Continuous secretion requires intact UPR machinery which helps adaptation to environmental changes through expansion of the ER, ER associated protein degradation and augmentation of the folding machinery. Totally these mechanisms improve the capacity of the secretory machinery for the high demand of protein production (Kaser et al., 2011). ER stress and autophagy are interconnected and ER stress is accompanied by autophagy under certain circumstances mostly as a survival mechanism (Gade et al., 2008; Kouroku et al., 2007; Sakaki and Kaufman, 2008).

1.5 Autophagy

The origin of the word autophagy comes from the Greek, meaning 'self-eating'. Autophagy is seen in normal cells at basal levels and provides balancing of the energy sources during development and proliferation. The process is thought to be a survival mechanism under conditions of nutrient limitation and also has a key in the clearance of damaged organelles and misfolded proteins through lysosomal degradation (He and Klionsky, 2009; Verfaillie et al., 2010). Three main types of autophagy are known: macro-autophagy, micro-autophagy and chaperone-mediated autophagy. Macro-autophagy, generally referred as autophagy, is the degradation of cytoplasmic components by the help of a membrane bound autophagosome fusing with the lysosome to form an autolysosome. Micro-autophagy on the other hand does not involve any autophagosome but the cytoplasmic components are directly engulfed by the lysosome. In chaperone mediated autophagy selected proteins are translocated through the lysosomal membrane by lysosomal-associated membrane protein 2A (LAMP-2A) (He and Klionsky, 2009).

The molecular mechanisms underlying autophagy (used instead of macro-autophagy throughout the text) have not been completely elucidated yet but several autophagy-related (*ATG*) genes were identified in the last decade. The Atg and other non-Atg proteins function coordinately at multiple steps during the process. These steps can be summarized as vesicle nucleation in which an isolation membrane (IM) is formed, vesicle elongation where the isolation membrane is converted into the autophagosome and the final step of the process is maturation; the formation of autolysosome. The constituents are degraded and recycled back into the cytoplasm (Gozuacik and Kimchi, 2004).

One of the key events in vesicle nucleation is the translocation of Atg9 from trans-Golgi to the autophagosome, which then promotes lipid recruitment to the expanding autophagophore. This movement is mediated by the activity of Ulk-1/Ulk-2 kinase (yeast Atg1) in complex with Atg13 and FIP200 (yeast Atg 17). The activity of this complex is regulated by mTORC1 (mammalian target of rapamycin complex 1) which inactivates Atg13 by phosphorylating it. Another important step in vesicle nucleation is the formation of phosphatidyl inositol triphosphate (PI3P) by a class III phosphatidylinositol 3 kinase (PI3K), vacuolar protein sorting 34 (Vps34), in complex with Beclin 1 (yeast Atg6). PI3P is essential for the trafficking of Atg9 and other Atg proteins in the newly forming phagophore.

Vesicle elongation involves two steps: Atg5–Atg12 conjugation and LC3 processing in which two ubiquitin like systems are in action. The first step includes the activation of Atg12 by E1 ubiquitin activating enzyme Atg7, its transfer to E2 like ubiquitin carrier protein Atg10 and conjugation to Atg5. The conjugated Atg5-Atg7, associate with Atg16L to form a larger complex which is thought to induce curvature to the growing phagophore membrane. This step is not dependent on autophagy and the complex dissociates when the autophagosome forms. The second ubiquitin like system involves the processing of microtubule-associated protein light chain 3 (MAPLC3, yeast Atg8). LC3 is first cleaved by Atg4 to create LC3-I (soluble),

activated by the E1 enzyme Atg7 and then is transferred to the E2 like protein Atg3. The last step is the lipidation of LC3 by the conjugation of phosphatidyl ethanolamine (PE) generating a membrane bound form, LC3-II. This process involves E3 like activity of Atg5-Atg12 complex. Lipidation is a reversible process and the amide bond between LC3 and PE is cleaved by Atg4, allowing LC3 to be recycled. LC3-II is found on both surfaces of the autophagosome and is essential for the elongation and closure of the membrane.

The final step in autophagy is the fusion of the autophagosome with the lysosome. LAMP2 and the small GTPase Rab7 are implicated in this process with additional Rab and soluble N-ethylmaleimide sensitive factor attachment protein receptor family (SNARE) proteins. The degradation of the autophagosomal content includes many lysosomal hydrolases like cathepsins B, D and L. The cytoplasmic content to be degraded was previously thought to be random; however, recent data suggest that specific proteins or organelles can be selectively degraded through autophagy. It is thought that LC3-II may act as a receptor acting coordinately with adaptor proteins like p62/SQSTM1 to promote selective uptake and degradation of certain proteins. The processes involved in autophagy are summarized in Fig. 1.4.
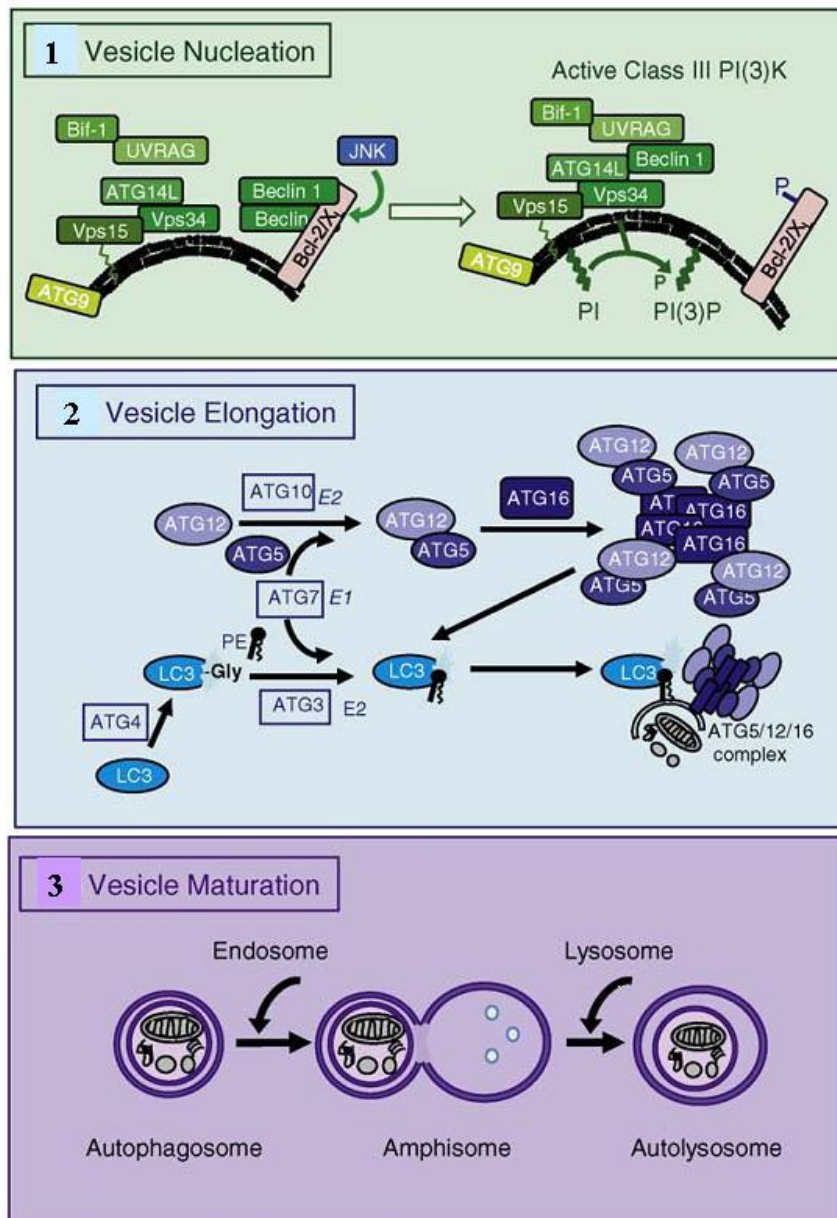
Fig. 1.4 Stages of autophagy (Shanmugam et al., 2012).

1.5.1 Signaling pathways regulating autophagy

Autophagy is regulated by several complex signaling pathways including nutrient related pathways (TOR and Ras/PKA), insulin/growth factor pathways, energy signalling (AMPK), stress response (ER stress, hypoxia, oxidative stress) and infection.

One of the key regulatory pathways in inducing autophagy is mTOR signalling since it acts as the major sensor of nutrients, energy and growth factors. mTOR phosphorylates and inactivates Atg13 and hence is a negative regulator of autophagy. mTOR is at the downstream of the Akt, PI3K, AMPK and growth factor receptor signaling pathways and is activated under growth stimulating conditions, repressing autophagy. Besides translation and cell cycle related proteins like 4EBP and p70S6K, the targets of mTOR includes Ulk1 and Atg13. The regulation of autophagy by mTOR signaling is shown in Fig. 1.5.
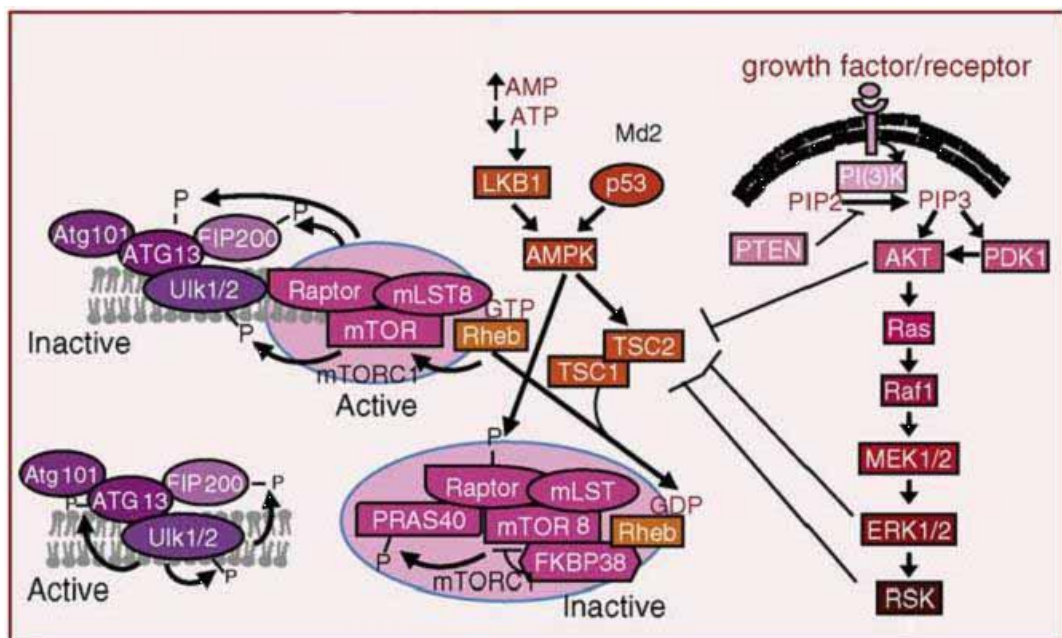
Fig. 1.5 Regulation of autophagy induction by mTOR (Shanmugam et al., 2012).

Another improtant level of regulation of autophagy is through the interaction of Beclin 1 with Bcl2/BclX$_L$. The B3 domain of Beclin 1 allows its interaction with these two antiapoptotic proteins. The interaction at the ER inhibits the activity of Beclin 1, which is disrupted by Jnk-1 mediated phosphorylation of Bcl2/BclX$_L$ under conditions of starvation (Fig. 1.4).

The regulation of protein translation by the phosphorylation of the eukaryotic translation initiation factor eIF2α has also been shown to be necessary for starvation induced-autophagy (Talloczy et al., 2002). When phosphorylated, the activity of eIF2α is inhibited and translation stops. However the translation of certain proteins, including bZIP transcription factors, continues, which is thought to be important for the transcription of autophagy related genes. The exact mechanism of how eIF2α regulates autophagy is not yet understood.

Another protein that is involved in the regulation of autophagy is death associated protein kinase (DAPK). DAPK is a serine-threonine kinase, which is dependent on calcium-calmodulin, associated with the cytoskeleton. Inhibition of DAPK and another close protein DRP1 results in the inhibition of autophagy (Bialik and Kimchi, 2006). Silencing of DAPK by promoter hypermethylation was reported in many types of cancer (Chakilam et al., 2013). STAT3 (Chakilam et al., 2013) and p52-NF-κB (Shanmugam et al., 2012) transcription factors have been shown to down-regulate DAPK expression. On the contrary, p53 (Martoriati et al., 2005), C/EBP-β (Gade et al., 2008) and Smad (Jang et al., 2002) transcription factors induce its transcription. DAPK has been shown to phosphorylate Beclin 1 and weaken its interactions with Bcl-2 and Bcl-X$_L$ (Zalckvar et al., 2009).

1.5.2 Autophagy and cancer

Although autophagy is thought to protect from genomic instability, prevent necrosis, induce cellular senescence and is implicated in promoting cell death (Degenhardt et al., 2006), it may also provide drug resistance and adaptation of tumor cells to stress as survival mechanisms (Amaravadi et al., 2007). For example Beclin 1 is deleted in

human ovarian, breast and prostate cancers thus showing tumour-suppressor properties (Liang et al., 1999). On the other hand, mice that are heterozygous for Beclin 1 are predisposed to cancer (Liang et al., 2006). Interestingly Li *et al.* (Li et al., 2009) showed that high Beclin 1 expression is mostly observed in stage III colorectal cancers and correlated with longer 5-year survival. It should also be mentioned that, autophagy eliminates damaged organelles such as mitochondria and peroxisomes, which may lead to the conclusion that autophagy protects a cell from apoptosis by cleaning up cytochrome c like molecules that would otherwise be released into the cytoplasm (Elmore et al., 2001). Hence the same process can be used as an adaptive mechanism to stress conditions. This was validated by Sato et al. (Sato et al., 2007) for colorectal cancer cell lines in which inhibition of autophagy led to apoptosis under nutrient deficient conditions.

Therefore the outcome of autophagy is highly dependent on the cellular context and the intensity and duration of the induction signals. Although a defect in basal autophagy results in the accumulation of protein aggregates, defects in stress-induced autophagy inhibit cell survival (Rabinowitz and White, 2010). Accordingly, autophagy has a dual role in cancer; as a tumor suppressor or providing tumor cell survival. The role of autophagy in tumorigenesis may vary among cancer types due to the different biological characteristics of cancer cells and their microenvironments.

1.5.3 Autophagy and differentiation

Autophagy is a crucial pathway in maintaining cellular homeostasis. It acts as a housekeeper under normal conditions to prevent cellular impairement. As has been mentioned earlier, a basal level of autophagy is present in all cells providing a quality control mechanism by a continuous turnover of cytoplasmic components. In addition, several studies show that autophagy is a key player in cellular differentiation. A central role of autophagy in differentiation was shown in adipogenesis. In 3T3-L1 preadipocytes and mouse models, autophagy was found to be necessary for adipocyte differentiation. Interestingly, this process is regulated by C/EBPβ, an important

transcription factor in adipocyte differentiation (Guo et al., 2013). Treatment of MCF-7 human breast cancer cells with the phytochemical pterostilbene resulted in activation of autophagy accompanied by epithelial like differentiation of these cells (Chakraborty et al., 2012).

Autophagy is of particular importance in the intestinal cells where there is continuous shedding of terminally differentiated apoptotic cells. Efficient corpse clearance through the activation of autophagy in the dead/dying or phagocytic cells may limit the development of inflammation (Levine et al., 2011). Loss of autophagy in the highly secretory Paneth cells of the small intestine was shown to result in defective secretory apparatus (Stappenbeck, 2010). There is little information in the literature on differentiation related autophagy in normal colon and colorectal cancer. In normal colon mucosa autophagy was found to be diminished from undifferentiated crypts to more differentiated villus (Groulx et al., 2012). In addition, Caco-2 and HT-29 colorectal cancer cell lines showed decreased levels of autophagy in their differentiated states (Groulx et al., 2012; Houri et al., 1995). Limiting Beclin 1 levels to basal levels was found to inhibit both autophagy and differentiation in leukemia cells which indicates a potential link between autophagy and differentiation (Wang, 2008). The mechanisms underlying the relationship between autophagy and differentiation are still to be elucidated.

1.6 Linking ER stress to autophagy

Accumulating evidence suggests that ER stress and autophagy pathways share some interconnections and may function together under certain circumstances. The ability of ER stress to trigger autophagy has now been shown in several studies (Gade et al., 2008; Kouroku et al., 2007; Sakaki and Kaufman, 2008). ER stress induced autophagy is generally a protective mechanism against cell death (Bernales et al., 2006; Kouroku et al., 2007). It has been proposed that when the protein degradation load is too high for the proteasomal machinery during UPR, autophagy is triggered and the lysosomal degradation system helps in the clearance of unfolded proteins. In

that context, Ogata *et al.* (Ogata et al., 2006) have shown that autopahgy inhibits thapsigargin or tunicamycin induced cell death. The molecular link between ER stress and autophagy and the consequences of the activation remains unclear.

The PERK-eIF2α branch of UPR was shown to mediate polyglutamine induced LC3 conversion and thus induce autophagy (Kouroku et al., 2007). The IRE1 arm of the UPR pathway was also shown to induce autophagy through JNK/TRAF2/JNK and thus modulating Beclin 1 function and expression (Verfaillie et al., 2010). Regulation of the mTOR pathway is one of the mechanisms that link ER stress and autophagy. ER is the major calcium storage site of the cell and Ca^{2+} release due to ER stress into the cytosol may activate autophagy through several mechanisms. Ca^{2+}/calmodulin-dependent kinase kinase β (CaMKKβ) is activated upon an increase in the cytoplasmic Ca^{2+} which activates AMPK and thus inhibits mTOR. Another Ca^{2+} activated kinase is aforementioned DAPK. The proposed pathways connecting ER stress and autophagy are summarized in Fig. 1.6.
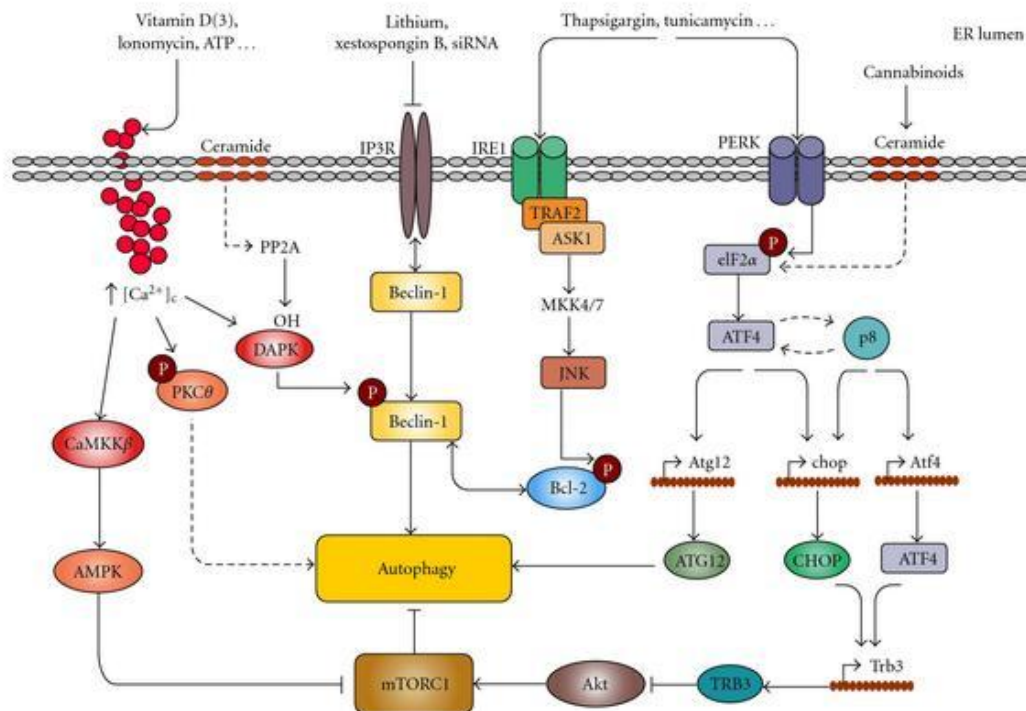
Fig. 1.6 Mechanisms connecting ER stress and autophagy (Verfaillie et al., 2010).

Therefore several intersection points exist between ER stress and autophagy and whether ER stress induced autophagy leads to survival or death is under debate. For example blocking autophagy in MEFs or in colonic cells inhibits cell death induced ER stress, whereas a similar inhibition in colon carcinoma cells results in an opposite phenotype; sensitivity to the ER stress (Ding et al., 2007). The consequence of autophagy activation upon ER stress may depend on the transformation status of the cells which should further be elucidated.

1.7   CCAAT/*E*nhancer *B*inding *P*rotein β (C/EBPβ)

C/EBPβ, which is implicated in cellular differentiation, proliferation, UPR, autophagy, apoptosis and immune responses, is one of the master regulators of

various cellular processes. It is one of the six members of the C/EBP transcription factors which are characterized by the basic-leucine zipper (bZIP) domain on their C-terminus. This domain is composed of a basic amino acid rich DNA-binding region and leucine zipper which functions in dimerization. The N-terminal transactivation domain, which interacts with the basal transcription apparatus, is more variable and excluded totally in some of the family members. All C/EBP isoforms share more than 90% sequence identity in their bZIP domain and therefore can form heterodimers in addition to homodimers with all family members and also with other bZIP containing proteins (Ramji and Foka, 2002).

Most strikingly, C/EBPβ has been widely implicated in the processes of cellular differentiation, ER stress and autophagy. C/EBPβ contributes to the differentiation of adipocytes (Lane et al., 1999), modulates the early events of keratinocyte differentiation, growth arrest and expression of differentiation markers (Zhu et al., 1999) and is upregulated in macrophage differentiation (Natsuka et al., 1992). However the expression and activity status of C/EBPβ in intestinal differentiation is not known. Additionally, C/EBPβ expression was shown to be induced during ER stress (Chen et al., 2004; Li et al., 2008; Meir et al., 2010) and a significant role in autophagy has also been proposed in several reports (Abreu and Sealy, 2010; Gade et al., 2008; Guo et al., 2013).

The mechanisms and the target genes of C/EBPβ provide an explanation of how this transcription factor may exert such varying functions. For example, antioxidant induced apoptosis was found to be mediated by induction of p21$^{WAF1/CIP1}$ by C/EBPβ in a p53 independent manner in colorectal cancer cells (Chinery et al., 1997). The autophagy related genes DAPK and Atg4b were shown to be transcriptionally upregulated by C/EBPβ (Gade et al., 2008; Guo et al., 2013). It has also been shown that C/EBPβ cooperates with Rb-E2F to implement Ras^{V12} induced cellular senescence by inhibiting E2F target genes and also interacting with Rb family proteins in primary fibroblasts (Sebastian et al., 2005). Yet another interesting finding was the existence of C/EBPβ-p65 (a subunit of NF-κB) complexes leading to

the inhibition of NF-κB activity in monocytic cells (Zwergal et al., 2006). Therefore C/EBPβ not only exerts its function through transactivation of target molecules but also through protein-protein interactions and the targets in intestinal epithelial differentiation are still to be elucidated.

The effects of this transcription factor on cellular proliferation are in fact controversial; it promotes both differentiation and tumor promotion (reviewed in (Nerlov, 2007)). For example, forced expression of C/EBPβ in hepatoma cells induces cell cycle arrest at G1–S (Buck et al., 1994) and systemic delivery of full-length C/EBPβ-liposome complex suppresses growth of human colon cancer in nude mice (Sun et al., 2005). On the other hand, ectopic C/EBPβ expression in a human mammary epithelial cell line (MCF10A) induces hyper-proliferation and the cells acquire a partially transformed phenotype (Bundy and Sealy, 2003) and it is also associated with cyclin-D1-dependent tumors (Lamb et al., 2003).

1.7.1 Regulation of C/EBPβ

C/EBPs are under several levels of control; transcriptional, translational, protein interactions, phosphorylation mediated changes in DNA binding activity, activation potential, nuclear localization and tissue/cell specific regulation (Ramji and Foka, 2002). One of the fundamental regulatory mechanisms of C/EBPβ is its translational control. Full length or short C/EBPβ isoforms arise by differential usage of translation initiation sites, which is mediated by an upstream open reading frame (uORF) conserved through evolution (Calkhoven et al., 2000). It has been proposed that a leaky scanning of ribosomes is responsible for the alternative use of three in-frame methionins, a mechanism observed during ER stress (please see section 1.4). Accordingly, C/EBPβ mRNA can give rise to three major isoforms: a 52 kDa protein C/EBPβ-3 (rat LAP*), a 45-48 kDa doublet C/EBPβ-2 (rat LAP) starting at 23 amino acids downstream of the first and a 20 kDa protein C/EBPβ-3 (rat LIP) starting at amino acid position 198 (Fig. 1.7).
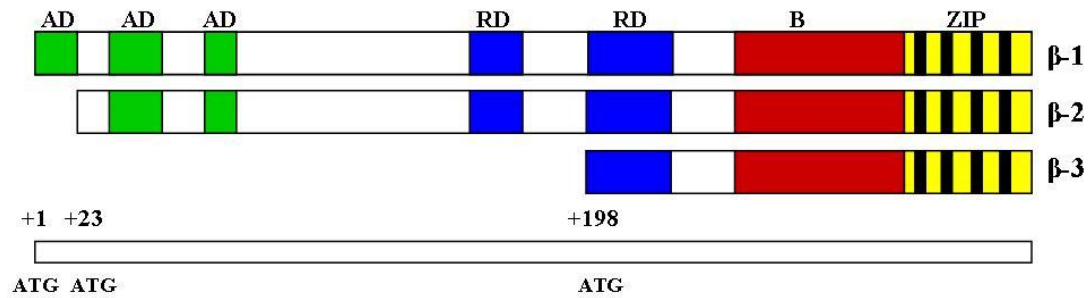
Fig. 1.7 Three isoforms of C/EBPβ. The leucine zipper; yellow-black, basic region; red, activation domains (AD); green and negative regulatory domains (RD); blue (adapted from (Ramji and Foka, 2002)).

The presence of several different isoforms of C/EBPβ may explain the functional controversy in the literature. The full length isoforms (LAP*/β1 and LAP/β2) are transcriptional activators as they both contain the activation domains. Although C/EBPβ-1 and β-2 are very similar in structure they were shown to have completely opposite functions. C/EBPβ-1 but not β-2 is able to recruit SWI/SNF chromatin remodelling complex which turns on differentiation related genes in myeloid cells (Kowenz-Leutz and Leutz, 1999). C/EBPβ-1 is expressed in non-transformed cells, however, β-2 expression is high in the majority of human breast tumors (Eaton et al., 2001). Lastly C/EBPβ-1 was shown to be involved in oncogene induced senescence (Atwood and Sealy, 2010). C/EBPβ-3 (LIP) isoform on the other hand, does not contain a transactivation domain and therefore has widely been thought to have an inhibitory effect on other isoforms as well as other bZIP family members. However, recently, it has been shown that LIP can bind to the promoter regions of the CXCR4 gene, leading to its transcriptional upregulation in breast cancer cells and enhanced metastasis (Park et al., 2013). It has also been shown that when overexpressed, LIP/β3 prevents proliferation arrest, interferes with terminal adipogenic differentiation and induces transformed phenotype (Calkhoven et al., 2000). On the other hand exogenous expression of C/EBPβ-3 has been shown to induce autophagy related cell death in breast cancer cells (Abreu and Sealy, 2010).

21

It can therefore be concluded from the current literature that the effect of C/EBPβ is highly context specific; it can promote or inhibit proliferation dependent on the cellular context and the isoforms present. The regulatory mechanisms in the differentiation-dedifferentiation of intestinal epithelial cells are unknown.

1.8   Scope and Aim of This Study

Understanding the cellular processes taking place during the differentiation of the intestinal epithelium has been the scope of a growing number of investigations because of the importance of these events in normal intestinal homeostasis, development and disease. However the differentiation process is a poorly understood phenomenon mostly due to the difficulties in handling primary cultures of the intestinal cells. In the current study the regulatory mechanisms underlying differentiation of the intestinal epithelium was aimed to be investigated, using two well established models, Caco-2 and HT-29 colorectal cancer cell lines.

CHAPTER 2

MATERIALS AND METHODS

2.1 Cell culture and differentiation

Caco-2 cells were purchased from ŞAP Enstitüsü (Ankara, Turkey) and grown in Eagle's minimum essential medium containing 1.5 g/L sodium bicarbonate, 1 mM sodium pyruvate, 12 mM L-glutamine, 0.1 mM non-essential amino acids, 20 % FBS and 1 % penicillin-streptomycin. In order to induce differentiation, cells were grown until confluency and the 100 % confluent cells were considered to be at day 0 for differentiation. The cells were grown three weeks after confluency and harvested at various intervals.

HT-29 cells were purchased from ŞAP Enstitüsü (Ankara, Turkey). Glucose deprivation by galactose substitution method established previously by Pinto et al. (Pinto et al., 1982) is used to induce differentiation in HT-29 cells. HT-29 cells were grown in DMEM medium containing 25mM glucose and 10% FBS (Glu-medium) and switched to DMEM medium without glucose, supplemented with 5mM Galactose and 10% dialyzed FBS (Gal-medium) when the cells were 80% confluent in order to induce differentiation. Cells were grown until confluency and the 100% confluent cells were considered to be at day 0. The cells were grown 20 days after confluency in Gal-medium and RNA and protein were isolated on regular intervals (Days 0, 2, 5, 7 and 10) for further experiments. All cell culture supplements were obtained from Biochrom (Berlin, Germany).

2.2   Treatments

Thapsigargin 1μM at 37°C for 6 h, BAPTA-AM 25 μM at 37°C for 3 h in Ca^{2+} free medium containing 3 mM EGTA, GSK2656157 1μM at 37°C for 1 h, rapamycin 5 μM at 37°C for 4 h.

2.3   RNA isolation and real time PCR

Total cellular RNA was isolated with RNEasy RNA Extraction kit (Qiagen, Hilden, Germany). 1 μg RNA was treated with DNase I enzyme (Fermentas, Vilnius, Lithuania) and reverse transcribed by RevertAid First Strand cDNA Synthesis kit (Fermentas) using oligo-dT primers and stored at -20ºC. Real time PCR reactions were performed in 10μl reaction volumes using FastStart Universal SYBR Green Master (Roche, IN, USA), 0.5 μM forward and reverse primers and 1 μl cDNA. Rotor GeneQ 6000 series (Qiagene) was used. Ct values were calculated using relative standard curve method and the fold change was calculated by Pfaffl method (Pfaffl, 2001). The primers used in the study are given in Table 2.1.

Table 2.1 Primer sequences and annealing temperatures used in this study.

Gene name	Accession number	Primer sequence	Amplicon length	Annealing temperature
Sucrase isomaltase	NM_0019413	5'-CAAATGGCCAAACACCAATG-3' 5'-CCACCACTCTGCTGTGGAAG-3'	160	59°C
Beclin-1	NM_003766.3	5'-TCACCATCCAGGAACTCACA-3' 5'- TTCAGTCTTCGGCTGAGGTT-3'	241	59°C
C/EBPβ	NM_0051942	5'-GACAAGCACAGCGACGAGTA-3' 5'-AGCTGCTCCACCTTCTTCTG-3	158	57°C
GAPDH	NM_0020463	5'-CGACCACTTTGTCAAGCTCA-3' 5'-CCCCTCTTCAAGGGGTCTAC-3'	238	60°C
XBP1	NM_005080.3	5'-TTACGAGAGAAAACTCATGGCC-3' 5'-GGGTCCAAGTTGTCCAGAATGC-3'	289 us 263 s	60°C

2.4   Protein isolation and Western blot

Total cellular proteins were isolated with M-PER Mammalian Protein Extraction Reagent (Thermo Scientific, IL, USA) containing 0.2 % NP-40 and protease inhibitor coctail. Protein amounts were determined with the Coomassie Plus reagent using the modified Bradford assay. Equal protein amounts were separated with 10-16 % SDS PAGE and electroblotted onto PVDF membranes (Roche). The membranes were blocked in 5% skim milk or 5% BSA for 1h at room temperature and were incubated overnight with the appropriate primary antibodies: ICAM-1 (1:300), VCAM-1 (1:250), E-cadherin (1:300), CEA (1:500), C/EBPβ (1:300), α-tubulin (1:500), β-actin (1:3000), TOPOIIβ (1:500), SERCA3 (1:500), SERCA2 (1:500) (Santa Cruz, CA, USA), phospho-mTOR (1:1000), phospho-eIF2α, phospho-eIF4E (1:1000) (Cell Signaling Technology, MA, USA), phospho-IRE1, (1:1000), (Abcam, Cambridge, UK), LC3 (1:1000) (Novus Biologicals, CO, USA) and p62 (Abnova, Taiwan) followed by incubation for 1h with a horseradish peroxidase–conjugated secondary antibody (1:2000). The membranes were visualized using the ECL Plus enhanced chemiluminescence kit (Pierce) according to the manufacturer's instructions.

2.4.1   Nuclear and cytoplasmic protein isolation

For the isolation of nuclear and cytoplasmic proteins, the cells were washed twice with ice cold PBS containing phosphatase inhibitor and resuspended in 500 μl of Hypotonic Buffer containing 10 mM HEPES pH 7.5, 4 mM NaF, 10 μM Na_2MoO_4, 0.1 mM EDTA, 1X Protease and phosphatase inhibitors (Roche) and incubated on ice for 15 min. Then 100 μl of 10% NP40 (Applichem) was added, mixed by pipetting and supernatants containing the cytoplasmic fraction were obtained by pulse centrifugation at highest speed for 30 sec. The remaining nuclear pellet was resuspended in 100μl of Nuclear Extraction Buffer containing 10 mM HEPES, pH7.9, 0.1 mM EDTA, 1mM DTT, 1.5 mM $MgCl_2$, 420 mM NaCl, 20% glycerol and with 1X protease and phosphatase inhibitors, incubated on ice for 30 min with

vortexing 15 sec in between. The lysate was centrifuged for 10 min at 14 000 x g at 4°C. The supernatant was considered as the nuclear fraction.

2.5   Alkaline phosphatase activity

The enzymatic activity of alkaline phosphatase was measured using p-nitrophenylphosphate as a substrate. 10 µl of total protein was mixed with 200 µl of substrate and incubated at room temperature in dark for 30 min. The absorbance at 405 nm was measured and the specific activity is calculated by dividing the absorbance values to the protein amount present in the samples.

The alkaline phosphatase activity was also determined by staining the cells with nitro blue tetrazolium chloride/ 5-bromo-4-chloro-3-indolyl phosphate p-toluidine (NBT/BCIP) salt. Briefly, the cells were washed twice with TBS, fixed in 70 % ethanol for 10 min, washed three times with TBS and then incubated with NBT/BCIP for 2 hr at room temperature in dark. The reaction is stopped by washing the cells with TBS and then the images were photographed.

2.6   Intracellular calcium measurement

Cells were grown in 25-cm^2 flasks, detached by 0.25% trypsin-EDTA and loaded with Fura-2/AM (a ratiometric fluorescent dye that binds to free intracellular calcium) for 45 min at 37°C in Ca^{2+}-standard buffer containing (mM): NaCl, 145; $MgCl_2$, 1; KCl, 5; $CaCl_2$, 1; glucose, 10; Hepes, 10 (pH 7.4). The cells were then centrifuged and resuspended in Ca^{2+}-standard buffer. After 15min of de-esterification at room temperature, the cells were washed three times in the same buffer.

Fluorescence was recorded from 100 µL aliquots of cells (1X10^6 cells/mL) at 37°C using Spectramax M5 microplate reader, Molecular Devices (UNAM, Bilkent University) with excitation wavelengths of 340 and 380 nm and emission at 510 nm. Background fluorescence was measured using same number of cells that are not loaded with Fura-2/AM and was subtracted from the measured fluorescence values

during the calculations. Changes in [Ca^{2+}] were monitored using the Fura-2 340/380 fluorescence ratio.

2.7   Reporter gene assays

In order to determine the changes in C/EBPβ activity in differentiating Caco-2 and HT-29 cells, C/EBP consensus sequence was cloned into pLuc-MCS luciferase vector (Stratagene, CA, USA) in three copies (A**TTGCGCAAT**)$_3$. Dual-Glo Luciferase assay system (Promega, WI, USA) was used. In order to transfect Caco-2 cells, Lipofectamine-LTX and Plus reagents (Invitrogen, USA), for the transfection of HT-29 cells, X-Treme gene (Roche) reagent was used. Caco-2 cells were grown in 6-well plates, pLuc-C/EBP firefly (0.5 μg/well) and phRL-TK (Promega, WI, USA) renilla luciferase vectors (0.005 μg/well) were diluted with Opti-MEM and PLUS reagent was added in 1:10 μg vector/μl reagent ratio. After incubating for 15 min, Lipofectamine-LTX reagent was added at the same ratio and incubated for 30 min. In the meantime, the cells to be transfected were washed with PBS and the culture medium was replaced with Opti-MEM. The transfection mixtures were added drop-wise and gently swirled. HT-29 cells were grown in 12-well plates, pLuc-C/EBP firefly (0.5 μg/well) and phRL-TK renilla luciferase vectors (0.05 μg/well) were diluted with Opti-MEM and X-Treme gene transfection reagent at a 1:3 ratio of μg vector/μl reagent. Afetr incubating 15 min at RT, the transfection mix was added dropwise.

In order to determine the luciferase activity, transfected cells were washed with PBS twice and harvested in 100μl Dual-Glo Luciferase Reagent for 10 min at room temperature. The harvested cells were centrifuged at 4°C at 14000 x g for 2min and supernatants were collected into 96-well white plates the luminescence values were read with lumiometer (Modulus, Turner Biosystems, USA). For renilla luciferase activity for normalization, 100μl Dual-Glo Stop&Glo Reagent was added to the wells and the measurements were taken after 15 min.

27

2.8 Chromatin Immunoprecipitation (ChIP)

Caco-2 and HT-29 cells were grown in 10 cm dishes. On the 0th, 10th and 20th days after reaching 100 % confluency, the culture medium was refreshed and 0.8 % formaldehyde was added to initiate the crosslinking, incubated at room temperature for 7 min and stopped by adding glycine to a final concentration of 125 mM. Cells were washed with PBS twice, scraped into 1.5 ml eppendorf tubes and centrifuged at 13000 x g for 1min at 4 °C. The pellets were then frozen in liquid nitrogen and then thawed in buffer A (200 M HEPES-KOH pH7.5, 420 mM NaCl, 0.2 mM EDTA pH 8.0, 1.5 mM $MgCl_2$, 25 % glycerol, 1X protease inhibitor). Thawed cells were incubated on ice for 20 min and centrifuged after which they were resuspended in breaking buffer (50 mM Tris-Cl pH 8.0, 1 mM EDTA pH 8.0, 150 mM NaCl, 1 % SDS, 2 % Triton X-100, 1X protease inhibitor) and sonicated with a probe sonicator for 12 cycles in 30 sec intervals of sonication and incubation on ice. After this, 50 μl inputs were taken and subjected to de-crosslinking (1hr RNaseA at 37°C, 1hr Proteinase K at 50 °C and o/n incubation at 60 °C) in buffer C (50 mM Tris-Cl pH 8.0, 1 mM EDTA pH 8.0, 150 mM NaCl, 0.1 % Triton X-100). Afterwards the inputs were ran on 1 % agarose gel to confirm the size of the sonicated fragments (200-1000 bp) and DNA amount was measured. Then the samples in buffer B were seperated so that each contained 25 μg DNA and were centrifuged at 13000 rpm for 10 min. The pellets were resuspended in Buffer C and 2.5 μg of antibody or isotype specific control IgG was added incubated at 4 °C with constant agitation o/n. The samples were then incubated with pre-blocked proteinA/G agarose beads (Santa Cruz,) for 2 hr at 4 °C with constant agitation and washed three times with wash buffer 1 (0.1 % SDS, 1 % Triton X-100, 2 mM EDTA pH 8.0, 150 mM NaCl, 20 mM Tris-Cl pH 8.0) and then with wash buffer 2 (0.1 % SDS, 1 % Triton X-100, 2 mM EDTA pH 8.0, 500 mM NaCl, 20 mM Tris-Cl pH 8.0). Samples were then eluted with elution buffer (1 % SDS, 100 mM $NaHCO_3$) and subjected to de-crosslinking as mentioned before. On the following day, DNA was isolated with high pure PCR product purification kit (Roche, Mannheim, Germany). Q-PCR was carried out with both immunoprecipitated and input samples using primers specific for the

promoters of the target genes. The primers used for ChIP studies are given in Table 2.2.

Table 2.2 Primer sequences used in ChIP experiments.

Gene name	Primer sequence	Amplicon length	Annealing temperature
Sucrase isomaltase	5'-GGCTGGTAAGGGTGCAATAA-3'	102	57°C
	5'-TGTTGTACCAGACTTGGATAAGG-3'		

2.9   Immunofluorescence and GFP-LC3 punctae analyses

Caco-2 cells were grown in 6-well plates and transiently transfected with 2.5 µg of pGFP-LC3 vector (obtained from Dr. Tamotsu Yoshimori, Department of Cell Biology, National Institute for Basic Biology, Okazaki, Japan (Kabeya et al., 2000)) for 48 h. As positive controls, cells were treated with rapamycin (5µM, 4h) or starved in HBSS (4h). The cells were then fixed in 4% formaldehyde for 15 min at RT, permeabilized in 0.3% Triton X-100 containing PBS for 10 min at RT and then stained with propidium iodide for 30 min at RT. Following this, cells were scraped and dispersed with mounting medium (Slow Fade Gold antifade reagent, Invitrogen) on glass slides. The cells were visualized using a fluorescence microscope (Leica, Wetzlar, Germany).

Quantitative analysis was done by counting individual transfected cells. Cells with at least five GFP-LC3 puncta were considered as autophagic. 100-200 GFP positive cells were counted for each replicate and the percentage of autophagic to the total GFP-positive cells were calculated.

2.10 Statistical Analyses

Data analysis and graphing was performed using the GraphPad Prism 5 software package (Prism, CA, USA). All experiments were repeated at least 3 times and data are expressed as mean ± SD. Statistical analyses between experimental results were based on one-way ANOVA using Dunnett's multiple comparison test or Students' t-test. Significant difference was statistically considered at the level of $p < 0.05$.

CHAPTER 3

RESULTS

3.1 Differentiation of Caco-2 and HT-29 cells

Spontaneous differentiation was induced in Caco-2 cells upon reaching 100% confluency whereas differentiation in HT-29 cells was attained by growing the cells in galactose containing medium (Gal-medium). The Caco-2 cells were monitored for 20 days after reaching confluency; HT29 cells were monitored for 10 days using an inverted microscope. Massive cell death was observed for both cell lines at the mid-stages of the process followed by the stabilization of the population. The undifferentiated, exponentially growing cells exhibited diffuse borders, however the edges become well limited and the cells acquired a polygonal shape in the differentiated cells, similar to the differentiated enterocytes of the intestinal epithelium. Domes, which are indicative of formation of tight junctions between the cells, started to appear in the early phases (Day 2-5) and were present during the whole process. Dome formation is caused by entrapment of fluids between the cells and the underlying surface, which in turn causes the local detachment of the monolayer (Fantini et al., 1986). Representative pictures for both cell lines in their undifferentiated and differentiated states, as well as the presence of domes are shown in Fig. 3.1.
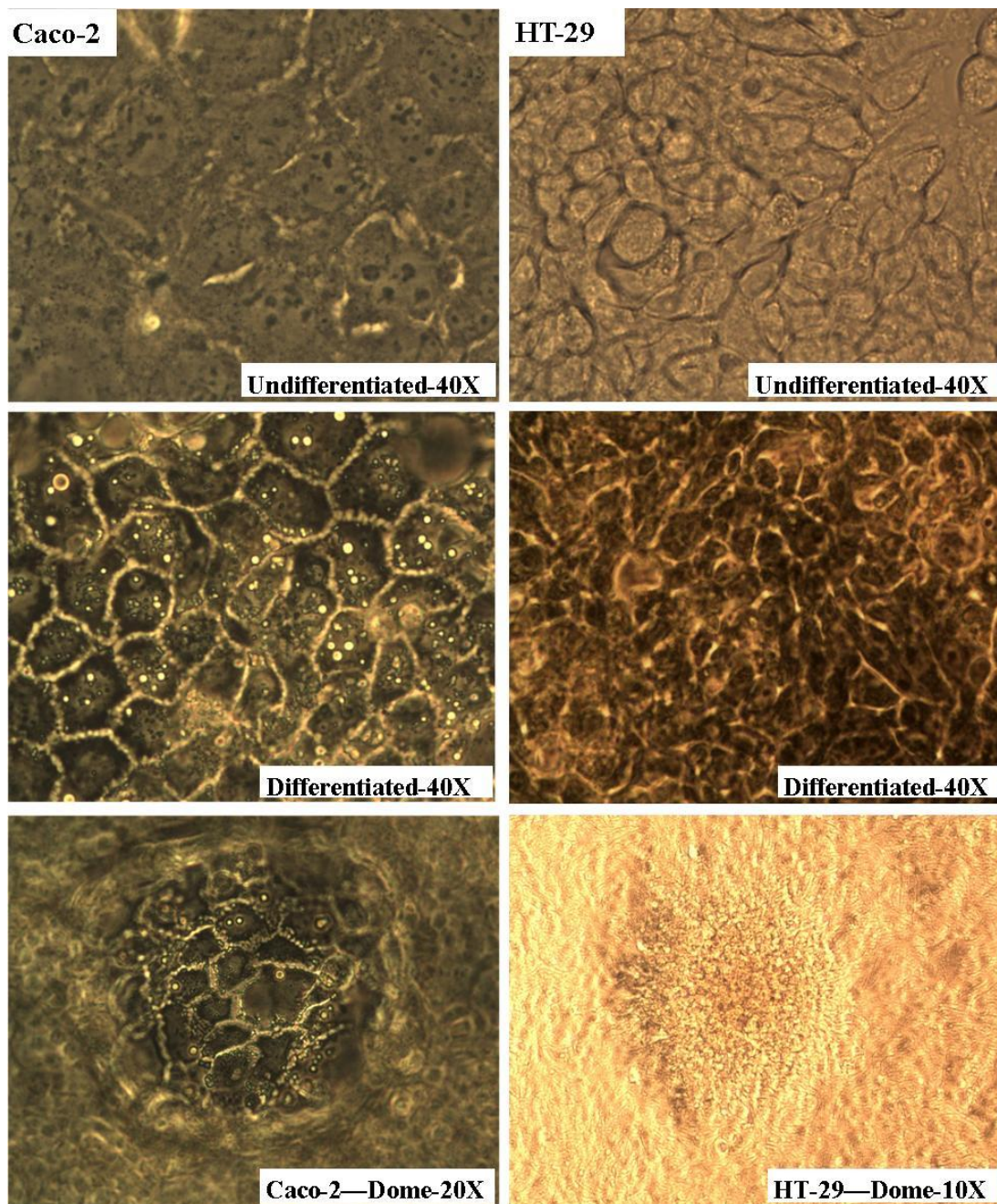
Fig. 3.1 Spontaneous differentiation of Caco-2 (left panel) and HT-29 (right panel) cells visualized under inverted microscope.

Differentiation of Caco-2 and HT-29 cells was confirmed by checking the mRNA and protein levels of common intestinal epithelial differentiation markers, sucrase isomaltase and carcinoembryonic antigen (CEA) by quantitative RT-PCR and western blotting, respectively. Another differentiation marker, alkaline phosphatase (ALP) activity was assessed colorimetrically using p-nitrophenylphosphate as a substrate as well as by NBT/BCIP staining (Fig. 3.2).

The results show that ALP enzymatic activity increases significantly for both cell lines (Fig 3A and B). The activity increased continuously for Caco-2 cells over 20 days however a peak on Day 5 then a decrease on Day 10 was observed for HT-29 cell line. The same trend was also observed in NBT/BCIP staining. Similar increases for sucrase isomaltase expression and protein levels of CEA also confirmed the differentiation process. Taken together, these results indicate that differentiation was successfully induced in both Caco-2 and HT-29 cell lines.
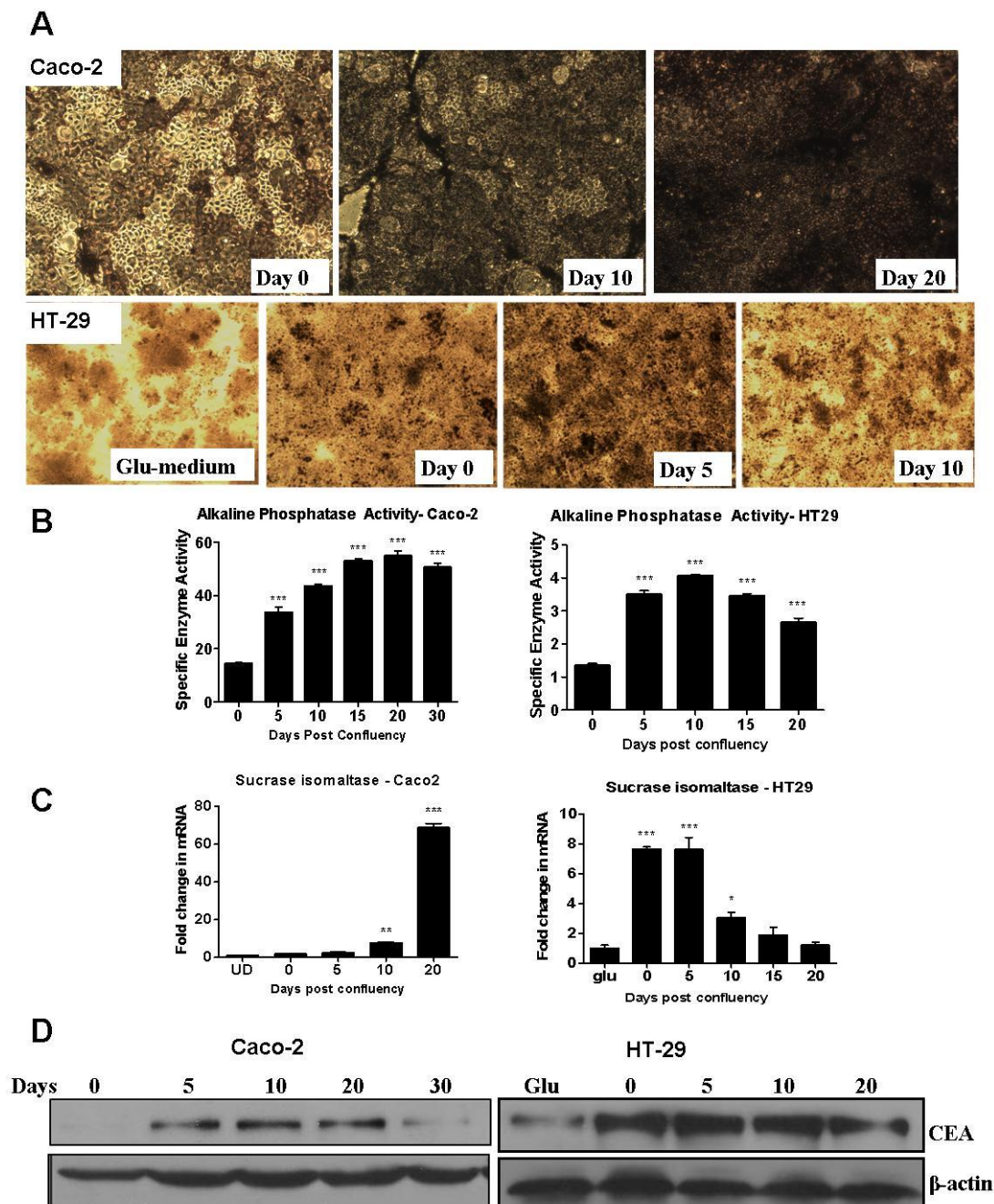
Fig. 3.2 Confirmation of differentiation in spontaneously differentiating Caco-2 and HT-29 cells shown by increasing alkaline phosphatase activity through (A) NBT/BCIP staining (B) pNPP colorimetric assay. Increase in sucrase isomaltase mRNA levels (C) and CEA protein levels (D) were other markers that confirmed the induction of differentiation. Figures are representative of three independent biological replicates. Bars represent mean ± SEM (n=3). *p<0.05, **p<0.01, ***p<0.001.

34

3.2 Cytoplasmic calcium levels in differentiating Caco-2 and HT-29 cells

Intracellular Ca^{2+} is one of the key regulators of cellular differentiation and growth. Increased cytoplasmic Ca^{2+} has been implicated in the differentiation of gastric cancer cells and in the normal intestinal epithelium (Lindqvist et al., 1998; Papp et al., 2004). To understand whether differentiation in Caco-2 and HT29 cells was also accompanied by changes in cytoplasmic Ca^{2+} levels, we used Fura2-AM, a ratiometric fluorescent dye that binds to Ca^{2+} (Fig. 3.3).
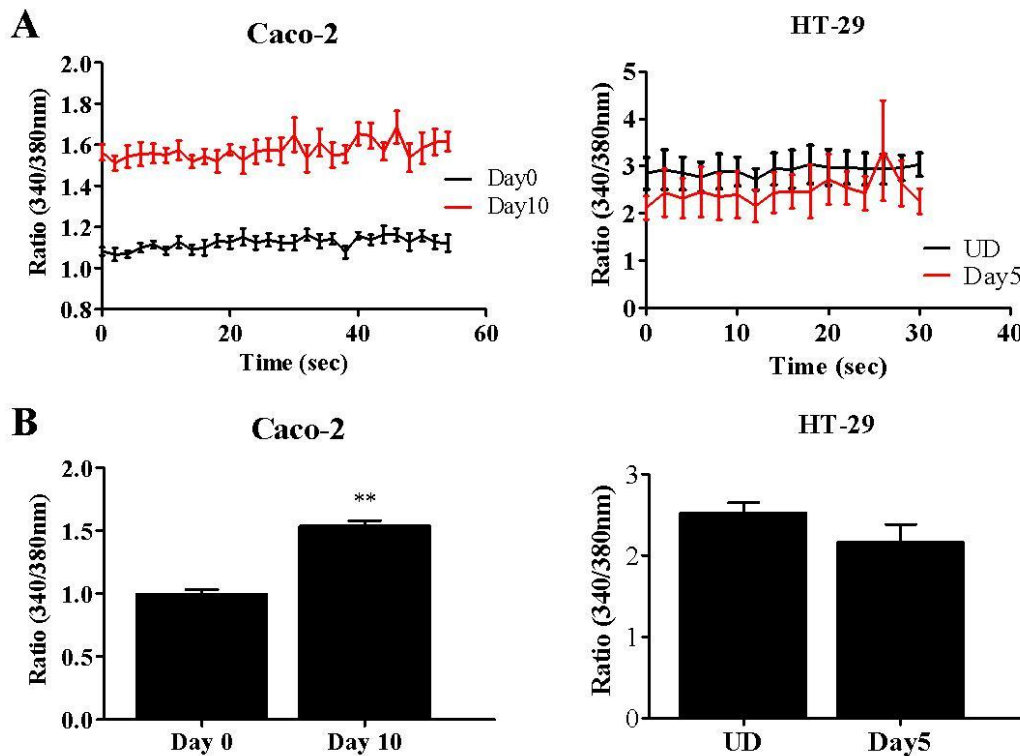
Fig. 3.3 Cytoplasmic calcium levels during differentiation of Caco-2 and HT-29 measured spectrofluorometrically using Fura2-AM. (A) Time course and (B) bar diagram analyses. Statistically significantly higher Ca^{2+} levels were seen in differentiated Caco-2 cells, but not in HT-29 cells. Bars represent average of two independent biological replicates with 5 technical replicates each, mean ± SEM. **$p<0.01$ (nested ANOVA).

In this method, fluorescence measured at 340 nm corresponds to the Ca^{2+} bound form of the dye and absorbances at 380 nm correspond to the free dye. The ratio of the fluorescence at these two wavelengths provides a method of normalization and cancels out the variability due to instrument efficiency and amount of dye in the cells (Grynkiewicz et al., 1985). Therefore the 340/380 nm ratio of the measured fluorescence is an indication of Ca^{2+} concentration in the cytoplasm of the cells. In Caco-2 cells a significant increase in the cytoplasmic Ca^{2+} on Day 10 compared to undifferentiated Day 0 cells was observed. However Ca^{2+} levels were not altered during HT-29 differentiation.

One of the possible reasons of the increase in cytosolic Ca^{2+} in differentiating Caco-2 cells is a change in the Smooth Endoplasmic Reticulum Ca ATPase (SERCA) expression during the process. We therefore checked SERCA2 and SERCA3 protein levels in both Caco-2 and HT-29 cells (Fig. 3.4).
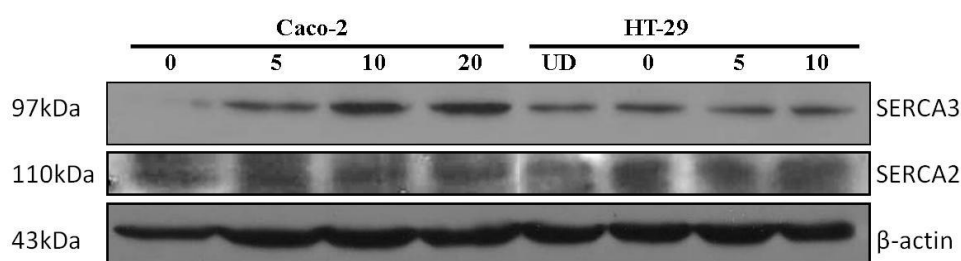
Fig. 3.4 Western blot showing the protein levels of the Ca ATPase SERCA2 and SERCA3 in the course of differentiation. An increase in protein levels of SERCA3, with low affinity for Ca, and no change in SERCA2 levels were observed.

Although SERCA2 protein levels do not change, that of SERCA3 increases during spontaneous differentiation of Caco-2 cells. On the other hand neither SERCA2 nor SERCA3 showed a change for HT-29 cells. Since SERCA3 has less affinity for Ca^{2+}

compared to SERCA2, increase in the levels of SERCA3 leads to lower Ca^{2+} entrapment in the ER leading to an increase in the cytosolic Ca^{2+} levels (Lytton et al., 1992). These results are consistent with Ca^{2+} measurements in which an increase in cytosolic Ca^{2+} in differentiating Caco-2 cells but no change in HT-29 was observed. The presence of a Ca^{2+} flux from ER to cytoplasm is usually accompanied by the generation of ER stress (Mahoney et al., 2012). Therefore we next examined whether the process of differentiation in Caco-2 cells was accompanied by the development of ER stress.

3.3   ER stress in differentiating Caco-2 and HT-29 cells

Decrease in the ER Ca^{2+} stores as well as glucose deprivation induces ER stress and UPR (Marciniak and Ron, 2006). Since cytoplasmic Ca^{2+} levels increased in differentiating Caco-2 cells and differentiation is induced directly by glucose deprivation in HT-29 cells we wanted to check common ER stress markers; phospho-IRE1 and its splicing of XBP1 and phospho-eIF2α in the cells (Fig. 3.5).
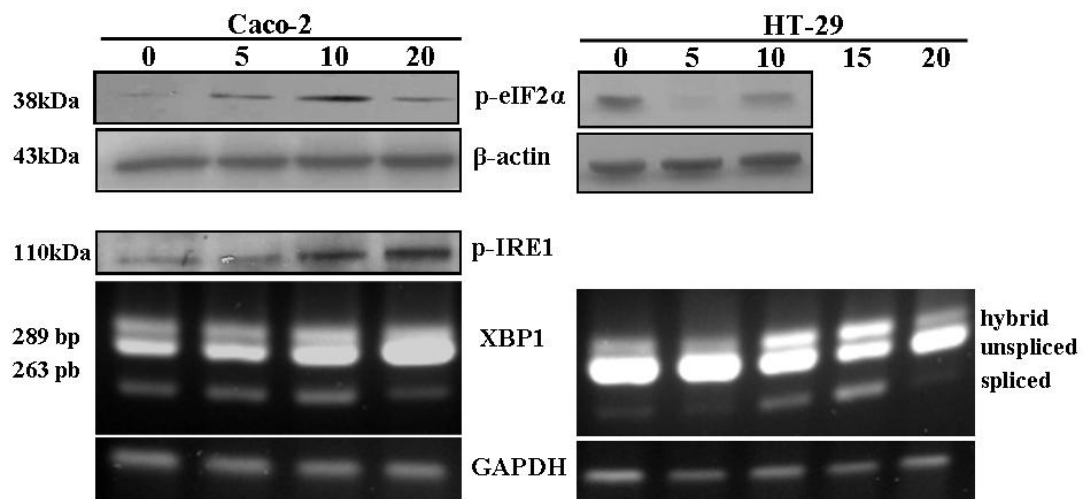
Fig. 3.5 ER stress is induced in differentiating Caco-2 and HT-29 cells. Top panel; phospho-eIF2α levels examined by Western blot, lower panel; pIRE1 protein levels by Western blot and splicing of XBP1.

eIF2α, when phosphorylated at Ser 51, loses its ability to bind to GTP and becomes inactivated during ER stress leading to a general shutdown of translation. The p-eIF2α levels showed an increase in differentiating Caco-2 cells at the mid-stages of the differentiation process (day 5 and day 10) and then decreased in the fully differentiated Day 20 cells. In HT-29 cells however, an opposite trend is observed for p-eIF2α; the phospho- form decreased at mid-stages and then increased at the end of the differentiation process.

The IRE1/XBP1 axis of the UPR pathway was also assayed in the differentiating Caco-2 and HT-29 cells. XBP1 is spliced by IRE1 forming unspliced (uXBP1) and spliced isoforms of XBP1 (sXBP1) which give 289 and 263 bp products, respectively. The slower migrating form is explained as a hybrid PCR product with one strand originating from the unspliced and the other from the spliced isoform (Back et al., 2006). XBP1 splicing was observed for both cell lines indicating an active IRE1, which was also confirmed by the increase in the phosphorylation of this protein at Ser 724. The results indicate that PERK/eIF2α axis is activated in Caco-2 but not in HT-29 cells, however, the IRE1/XBP1 axis is activated in both cell lines. Therefore the ER stress response is activated during differentiation for both Caco-2 and HT-29 albeit through different mechanisms.

3.3.1 Relationship of calcium and ER stress in differentiating Caco-2 cells

In order to understand if the increase in cytoplasmic Ca^{2+} was responsible for triggering the activation of ER stress response in spontaneously differentiating Caco-2 cells, the phosphorylation of eIF2α at Ser51 was examined in the presence of the SERCA inhibitor thapsigargin, intracellular Ca^{2+} chelator BAPTA-AM and PERK inhibitor GSK2656157.
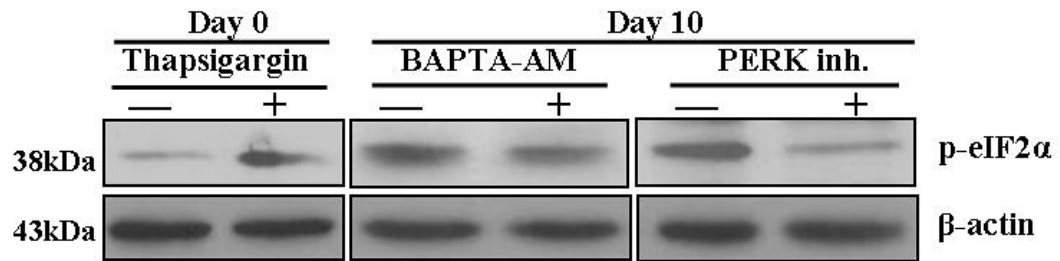
Fig. 3.6 phospho-eIF2α levels in Caco-2 cells in the presence of the SERCA inhibitor thapsigargin (1 µM), cytoplasmic Ca^{2+} chelator BAPTA-AM (25 µM) and PERK inhibitor GSK2656157 (1 µM) examined by Western blot. Treatment with thapsigargin in the undifferentiated Day 0 Caco-2 cells resulted in the induction of ER stress. Day 10 cells, which have ER stress, showed a reversal in the phosphorylation of eIF2α when Ca^{2+} was chelated or PERK was inhibited.

In order to mimic the proposed mechanism of SERCA3 induced Ca^{2+} release in the cytoplasm, undifferentiated Caco-2 cells were treated with a specific SERCA inhibitor thapsigargin, which prevents the reuptake of Ca^{2+} from the cytoplasm. eIF2α phosphorylation was increased, indicating induction of ER stress response, when SERCA pumps were inhibited by thapsigargin. In the differentiated Caco-2 cells (Day 10), which already exhibit ER stress, treatment with BAPTA-AM or a PERK inhibitor resulted in the opposite effect, in which phosphorylated eIF2α levels fell, indicating a relief from ER stress. Chelating Ca^{2+} with BAPTA-AM was not as effective as the inhibition of PERK, which rescued the phenotype completely, suggesting more diverse mechanisms for BAPTA-AM. Inhibition of PERK in differentiated cells on the other hand resulted in p-eIF2α levels similar to that of undifferentiated day 0 cells.

Since ER stress frequently leads to cell death mechanisms such as autophagy (Gade et al., 2008; Kouroku et al., 2007; Sakaki and Kaufman, 2008), and both ER stres and autophagy have been implicated in the differentiation process (Chakraborty et al., 2012; Guo et al., 2013; Kaser et al., 2011; Liu et al., 2012; Sugiura et al., 2009), we

decided to examine whether autophagy is induced in the two models of intestinal differentiation.

3.4 Autophagy in differentiating Caco-2 and HT-29 cells

In order to determine autophagy in differentiating Caco-2 and HT-29 cells common autophagy markers, LC3 and p62 were examined by Western blot (Klionsky et al., 2012) (Fig. 3.7).
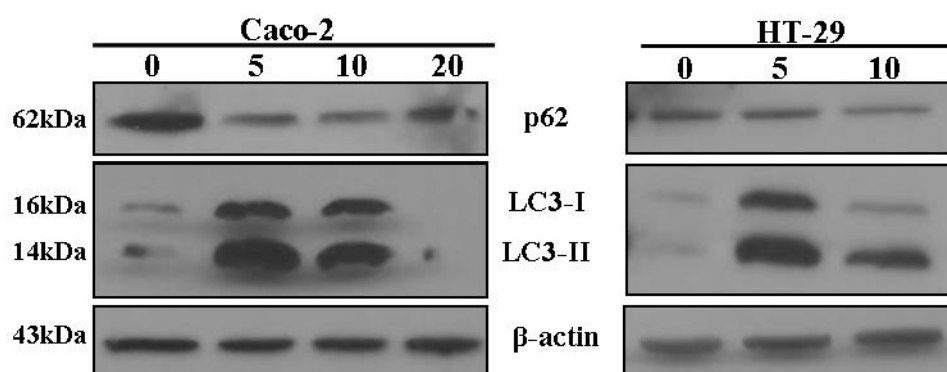
Fig. 3.7 The autophagy markers LC3 and p62 were examined by Western blot in spontaneously differentiating Caco-2 and HT-29 cells. p62 is the adapter protein that is degraded by the lysosome together with its cargo indicating autophagic flux. Phosphatidylethanolamine (PE) conjugated LC3-I is LC3-II which interacts with the autophagosomes.

LC3-I is the soluble form of the protein that is present in the cytoplasm whereas LC3-II is the phosphatidylethanolamine (PE) conjugated, membrane associated form which interacts with the autophagosomes. An increase in both LC3-I and II is observed in the mid-stages of the differentiation process in both Caco-2 and HT-29 cells. This indicates an increase in both amount and the rate of LC3-I conversion to LC3-II leading to autophagosome accumulation. This increase may result from two

possibilities; either the degradation machinery may be defective so that the autophagosomes are not cleared effectively or the autophagy machinery may be correctly working but the rate of autophagosome formation is high. Therefore information on the autophagic flux is of particular importance. This can be monitored through the p62 adapter protein, which interacts with LC3-II at the autophagosomes and is degraded together with its cargo protein (Klionsky et al., 2012). A decrease in the steady state levels of p62 is an indicator of active autophagy machinery. During the course of differentiation of both Caco-2 and HT-29, p62 levels showed a decrease indicating an increase in the autophagic flux.

In order to further confirm the occurrence of autophagy in differentiating Caco-2 cells, the mRNA expression of beclin-1,another marker of autophagy, was determined by qPCR.
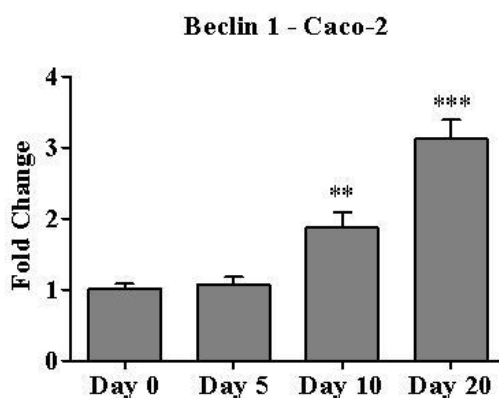
Fig. 3.8 Beclin-1 expression in spontaneously differentiating Caco-2 cells determined by qPCR. A significant increase in the mRNA levels was seen in Day 10 and 20 after reaching confluence. Each bar represents average of three independent experiments, mean ± SEM. **p<0.01, ***p<0.001 (nested ANOVA).

Additionally, the presence of LC3-II associated autophagosomes was confirmed by the formation of GFP-LC3 punctae via immunofluorescence.
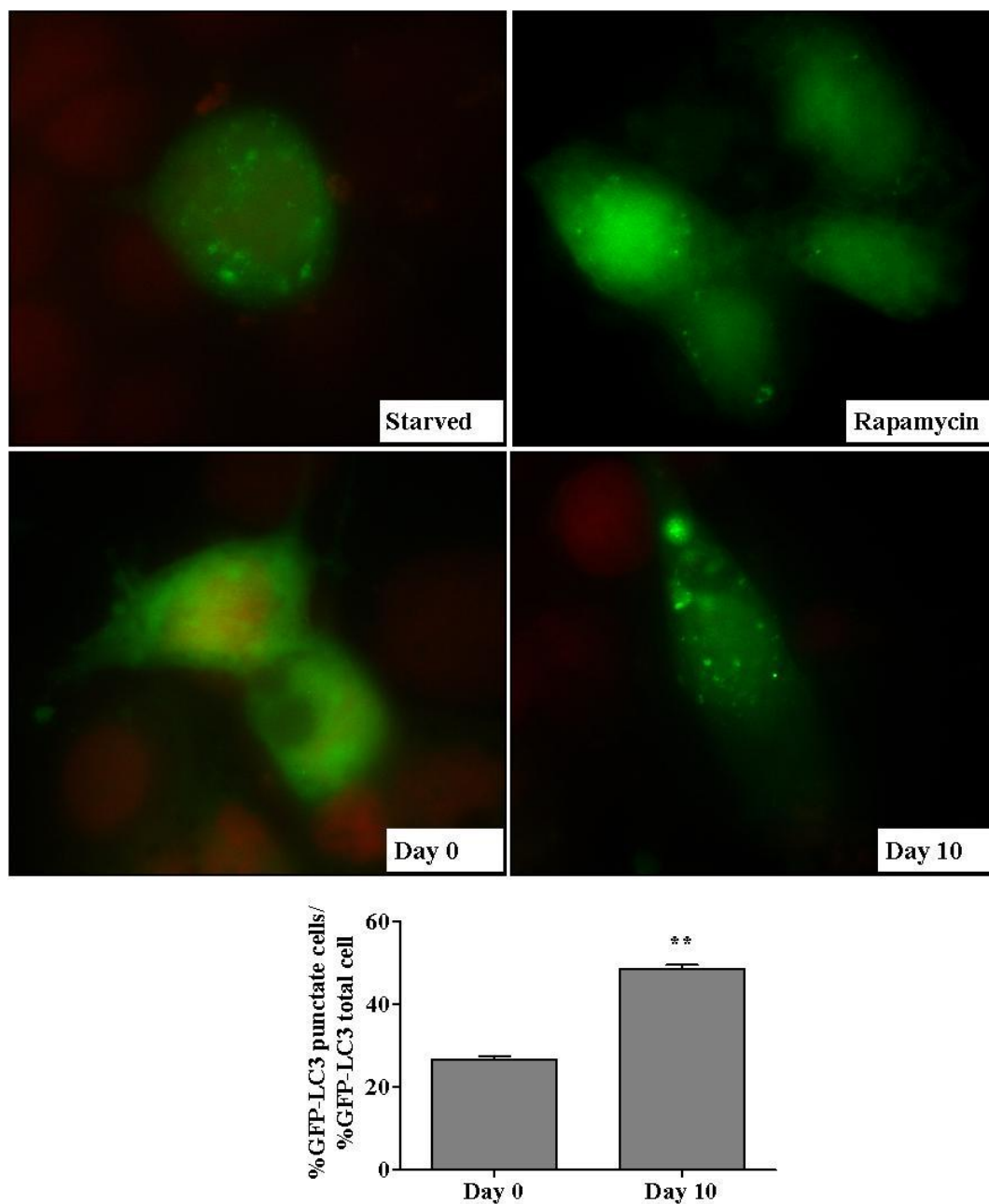
Fig. 3.9 GFP-LC3 punctae formation in differentiating Caco-2 cells. Cells transiently transfected with GFP-LC3 plasmid for 48h, treated with rapamycin (5µM, 4h) or starved in HBSS (4h) as positive controls examined by fluorescence microscopy. (**top**) The picture shows a representative image from two independent experiments with two replicates each visualized with 100X objective. (**bottom**) Quantitative

analysis of GFP-LC3 cells. The percentage of GFP-positive cells with at least five GFP-LC3 puncta was calculated (n>100), bars represent mean±S.D, **p<0.05 (Nested ANOVA).

When autophagy was induced, the GFP-LC3 molecules were recruited to the autophagosomes appearing as bright dots under fluorescent microscope. The cells bearing at least five dots were accepted as autophagic since a basal level of autophagy is present in normal cells (He and Klionsky, 2009). The number of cells containing GFP-LC3 punctate increased significantly on day 10 (48.8%) compared to day 0 (26.6%) confirming the increase in autophagy.

3.4.1 Calcium and autophagy in differentiating Caco-2 cells

Since calcium flux into the cytoplasm was responsible for the induction of ER stress in Caco-2 cells we wanted to determine if autophagy was also induced downstream of this axis. LC3I and II levels were determined in the presence of the SERCA inhibitor thapsigargin, Ca^{2+} chelator BAPTA-AM and PERK inhibitor GSK2656157.
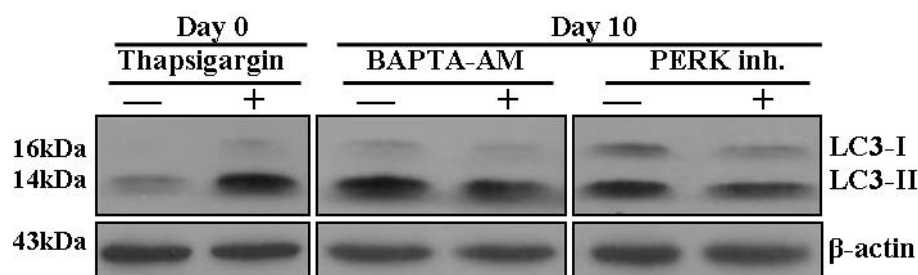
Fig. 3.10 LC3I conversion to LC3-II by phosphatidylethanolamine (PE) conjugation indicating autophagosome formation in spontaneously differentiating Caco-2 cells in the presence of the SERCA inhibitor thapsigargin (1 μM), Ca^{2+} chelator BAPTA-AM (25 μM) and PERK inhibitor GSK2656157 (1 μM).

When the SERCA pumps are inhibited and more Ca^{2+} is retained in the cytoplasm in the undifferentiated cells, a marked increase in LC3-II is observed. The opposite effect is also seen with the Ca^{2+} chelator BAPTA-AM and PERK inhibitor in day 10 differentiating cells although the effect is not completely reversed back to day 0 levels. These results suggest a role for Ca^{2+} flux from the ER into the cytoplasm in the induction of autophagy. However Ca^{2+} probably is not the only mechanism in action since chelating it or inhibiting the PERK/eIF2α axis do not completely rescue the phenotype.

To explain the molecular mechanisms linking ER stress to autophagy, it was hypothesized that C/EBPβ, a transcription factor implicated in both processes in addition to differentiation may be involved in coordinating these diverse cellular processes.

3.5   C/EBPβ in differentiating Caco-2 and HT-29 cells

The mRNA and protein levels of C/EBPβ were first determined in differentiating Caco-2 and HT-29 cells (Fig. 3.11).
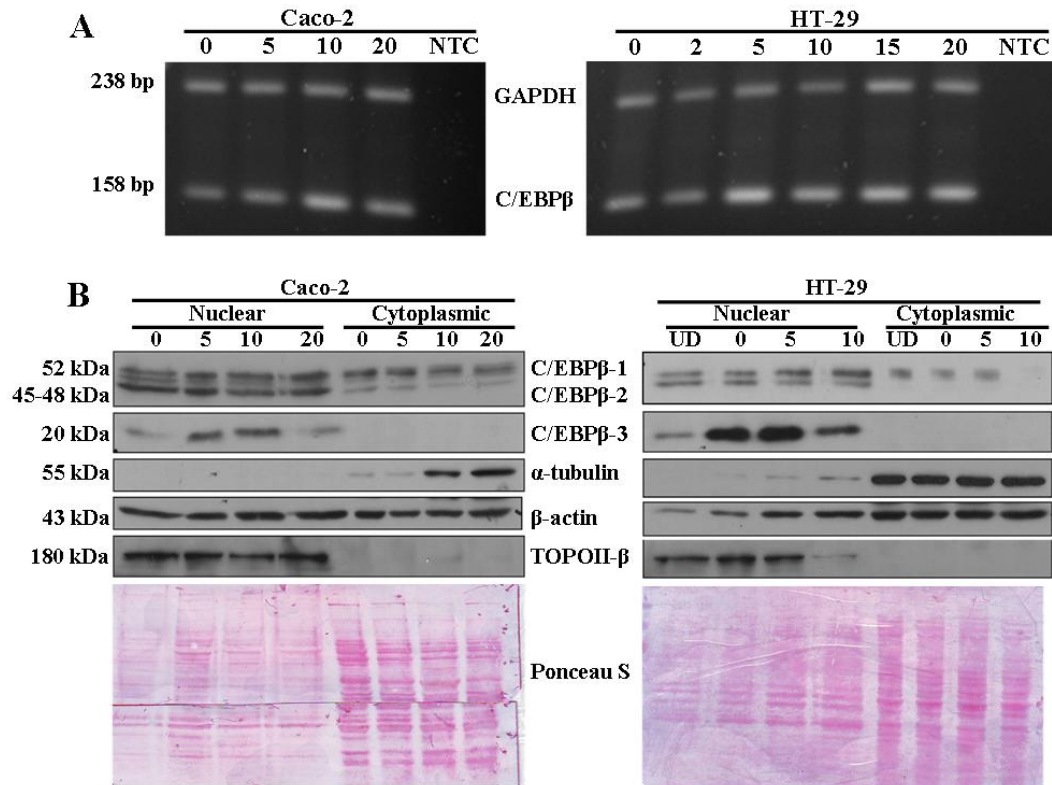
Fig. 3.11 mRNA (**A**) and protein (**B**) levels of C/EBPβ in differentiating Caco-2 and HT-29 cells. Each picture is a representative of three independent biological replicates.

The mRNA levels of C/EBPβ increased in the mid-stages of differentiation in both cell lines, albeit very slightly. One of the fundamental regulatory mechanisms of C/EBPβ is its translational control. The protein amounts of the three isoforms of C/EBPβ that are generated through alternative translation, showed variations during differentiation in both cell lines. There was no significant change in C/EBPβ-1 (52 kDa) and C/EBPβ-2 (45-48 kDa doublet) for both cell lines. Interestingly, C/EBPβ-3 showed a remarkable increase at the mid-stages of the differentiation process and then decreased in the fully differentiated cells, indicating that this isoform could be a major player in these cell lines.

45

3.5.1 ER stress and C/EBPβ-3

The regulation of C/EBPβ-3 through the phosphorylation and inactivation of the translation initiation factors eIF2α and eIF4E has previously been shown (Calkhoven et al., 2000). The timing of the C/EBPβ-3 increase in Caco-2 cells coincides with the increase in p-eIF2α levels (days 5 and 10) suggesting an association between these events. In order to further elucidate the relation of Ca^{2+} induced ER stress and C/EBPβ-3, the protein levels of this short isoform were determined in the presence of the SERCA inhibitor thapsigargin, Ca^{2+} chelator BAPTA-AM and PERK inhibitor GSK2656157 (Fig. 3.12).
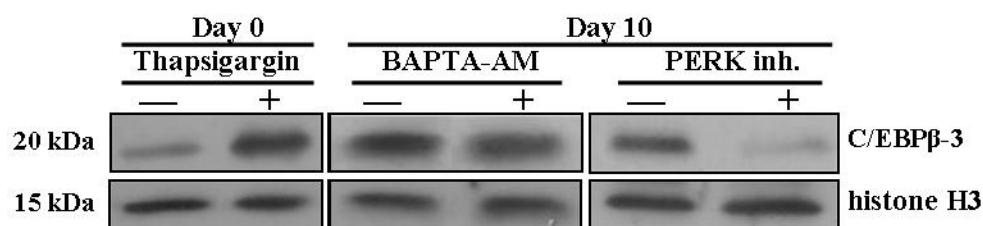
Fig. 3.12 C/EBPβ-3 protein levels in spontaneously differentiating Caco-2 cells in the presence of SERCA inhibitor thapsigargin (1 μM), Ca^{2+} chelator BAPTA-AM (25 μM) and PERK inhibitor GSK2656157 (1 μM).

The SERCA inhibitor thapsigargin caused a marked increase in C/EBPβ-3 in undifferentiated day 0 cells. In addition, the extent of the increase was similar to the one seen on Day 10 cells. Chelating Ca^{2+} with BAPTA-AM decreased C/EBPβ-3 in day 10 differentiating cells although the decrease was not so profound. A more robust inhibition with the PERK inhibitor GSK2656157 lowered C/EBPβ-3 protein to similar levels with undifferentiated cells. Therefore C/EBPβ-3 production is dependent on Ca^{2+} flux into the cytoplasm. In addition, inhibiting the PERK/eIF2α

axis leads to the inhibition of C/EBPβ-3 suggesting that C/EBPβ-3 was acting downstream of this axis.

As the phosphorylation of eIF2α in HT-29 cells was decreased, this protein was not involved in the increase in C/EBPβ-3 protein in these cells. Another translation initiation factor, eIF4E, which is implicated in C/EBPβ-3 regulation, was therefore checked during the differentiation process of Caco-2 and HT-29 cells (Fig. 3.13).
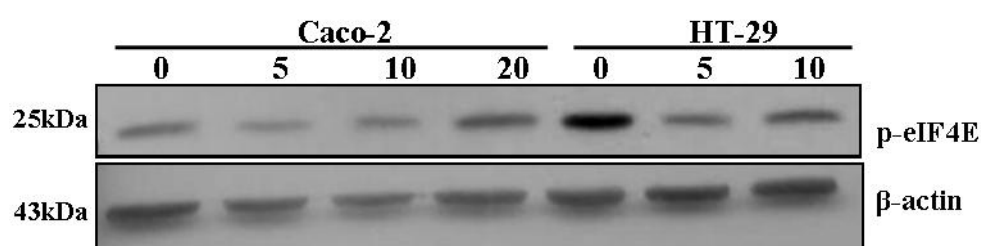
Fig. 3.13 phospho-eIF4E levels in differentiating Caco-2 and HT-29 cells determined by Western blot.

eIF4E phosphorylation is an indication of translational activity and a high level of p-eIF4E in undifferentiated HT-29 cells when compared to Caco-2 cells was observed. The levels fell down remarkably on day 5 and slightly increased on day 10 in HT-29 cells. In Caco-2 cells however the changes in p-eIF4E were not as pronounced as HT-29. The decrease in phosphorylation on day 5 coincides with the increase in C/EBPβ-3 protein on the same day, suggesting a regulatory mechanism for C/EBPβ-3 through eIF4E in HT-29 cells.

3.5.2   C/EBPβ-3 and Autophagy

The temporal increase in C/EBPβ-3 corroborates with the increase in autophagy in Caco-2 cells. In order to understand whether autophagy was induced by C/EBPβ-3, undifferentiated Caco-2 cells were transiently transfected with pCMV-C/EBPβ-3 vector and LC3 levels were determined after the expression of C/EBPβ-3 was confirmed by Western blot (Fig. 3.14).
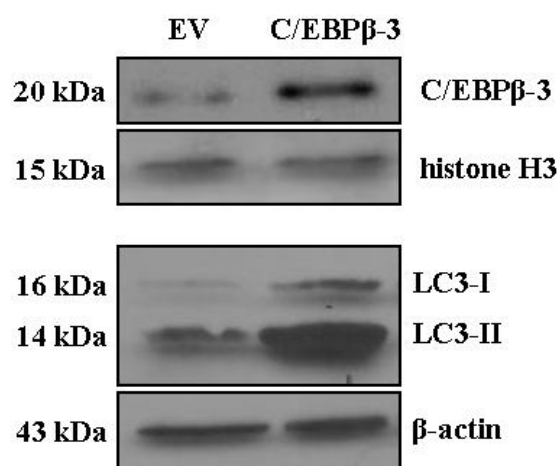
Fig. 3.14 Induction of autophagy (indicated by the high levels of LC3-II) in Caco-2 cells overexpressing C/EBPβ-3. EV; empty vector.

The results show that LC3-II formation increases in cells overexpressing C/EBPβ-3, indicating a role for C/EBPβ-3 in the induction of autophagy. In addition, p-eIF2α levels were also checked in the transfected cells in order to determine if C/EBPβ-3 is able to induce ER stress (Fig. 3.15).
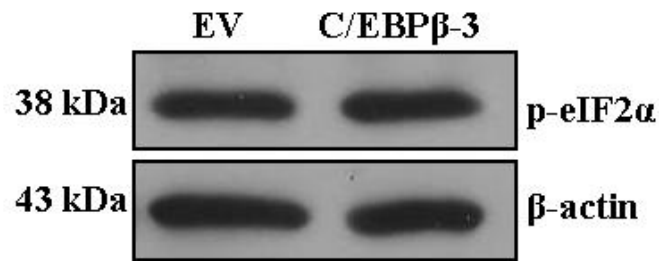
Fig. 3.15 phospho-eIF2α levels in Caco-2 cells showed no change when C/EBPβ-3 was overexpressed, indicating that this protein acted upstream of C/EBPβ-3.

There was no difference in the phosphorylated levels of eIF2α in the C/EBPβ-3 overexpressing cells compared to the empty vector transfected cells. These results suggest a role for C/EBPβ-3 downstream of PERK/eIF2α axis of the ER stress and upstream of LC3-II conversion of the autophagy pathways.

3.5.3 Transcriptional activity of C/EBPβ

C/EBPβ-3 may exert its function either by increasing the transcription of autophagy inducing genes or by decreasing the genes that are inhibitors of autophagy. In order to examine how C/EBPβ-3 induces LC3 conversion, the transcriptional activity of C/EBP was first determined by luciferase reporter assays using pLUC-C/EBP vector (Fig. 3.16).
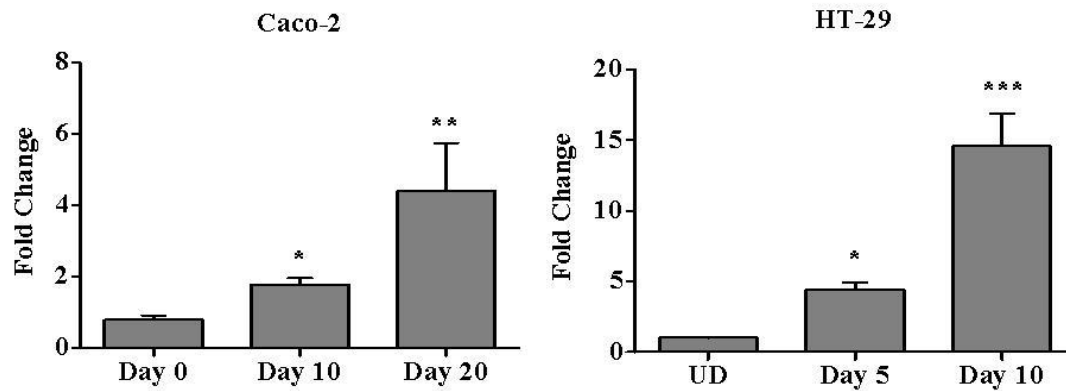
Fig. 3.16 C/EBP transcriptional activity in differentiating Caco-2 (left) and HT-29 (right) cells. Each bar represents average of at least three independent biological replicates, mean±SEM (ANOVA). *p<0.05, **p<0.01, ***p<0.001

The transcriptional activity of C/EBP was found to increase during spontaneous differentiation of both Caco-2 and HT-29 cells. The transcriptional activity was also assessed in pCMV-C/EBPβ-3 transfected Caco-2 cells.
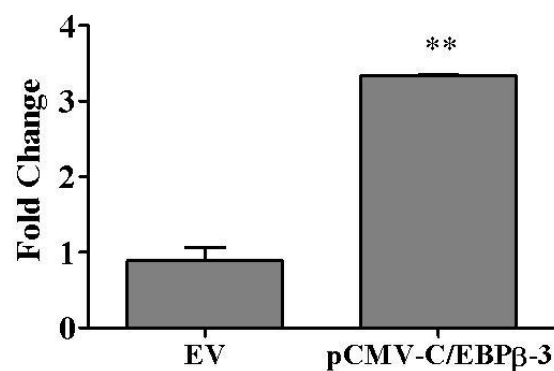
Fig. 3.17 C/EBP activity showed an increase in pCMV-C/EBPβ-3 transfected Caco-2 cells. Each bar represents mean±SEM (paired t-test), **p<0.01.

Overexpression of C/EBPβ-3 resulted in an increase in the activity of C/EBP transcription. It is interesting to see this increase in the transcriptional activity of C/EBP since C/EBPβ-3, without the transactivation domain, is thought to be a transcriptional repressor. It is necessary to note that the pLUC-C/EBP vector contains three consecutive C/EBP consensus binding sequences and any C/EBPβ isoform as well as other members of the C/EBP family may bind to this consensus sequence. Therefore we confirmed the specific binding of C/EBPβ to its target promoter sequences by chromatin immunoprecipitation (ChIP).

ChIP assays were carried out using a C/EBPβ antibody that can recognize all three isoforms of C/EBPβ. Binding of C/EBPβ to the promoter of sucrase isomaltase, a known target of C/EBPβ and a marker of differentiation, was investigated. A 1000 bp region of the sucrase isomaltase promoter was analyzed by three different databases, namely, alibaba2 (Biobase, http://www.gene-regulation.com/pub/programs/alibaba2/index.html, last visited on January 2014), Match 1.0 (Biobase, http://www.gene-regulation.com /cgi-bin/pub/programs /match/bin/match.cgi, last visited on January 2014) and TFSearch (Computational Biology Research Center, http://www.cbrc.jp/ research/db/TFSEARCH.html, last visited on January 2014). Five sites were detected by at least two of the programs dispersed throughout this region. Primers were designed for the most proximal region with respect to start site of the promoter.
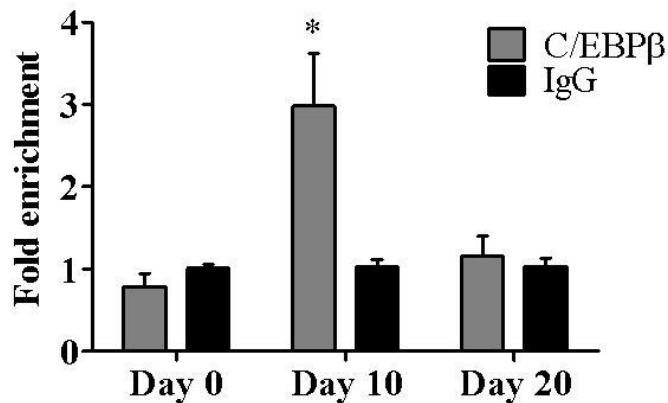
Fig. 3.18 Sucrase isomaltase promoter binding of C/EBPβ in differentiating Caco-2 cells. Each bar represents average of three independent biological replicates, mean ± SEM. * $p<0.05$, compared to Day 0.

C/EBPβ enrichment on sucrase isomaltase promoter increases significantly on day 10. Since there is no antibody that can bind solely to C/EBPβ-3, all three isoforms may be responsible for this increase. However the trend, increased binding in mid-stages of differentiation and then decrease on day 20, corroborates with the nuclear levels of C/EBPβ-3, which indicates that this specific isoform may be binding to the promoter.

3.5.4 Autophagy related targets of C/EBPβ

Several autophagy related targets of C/EBPβ has been implicated in the literature. In order to determine some targets cluster analyses of autophagy related genes was done from a publicly available microarray data for differentiating Caco-2 cells (GDS709). Among these, possible targets of C/EBPβ implicated in the literature are given in
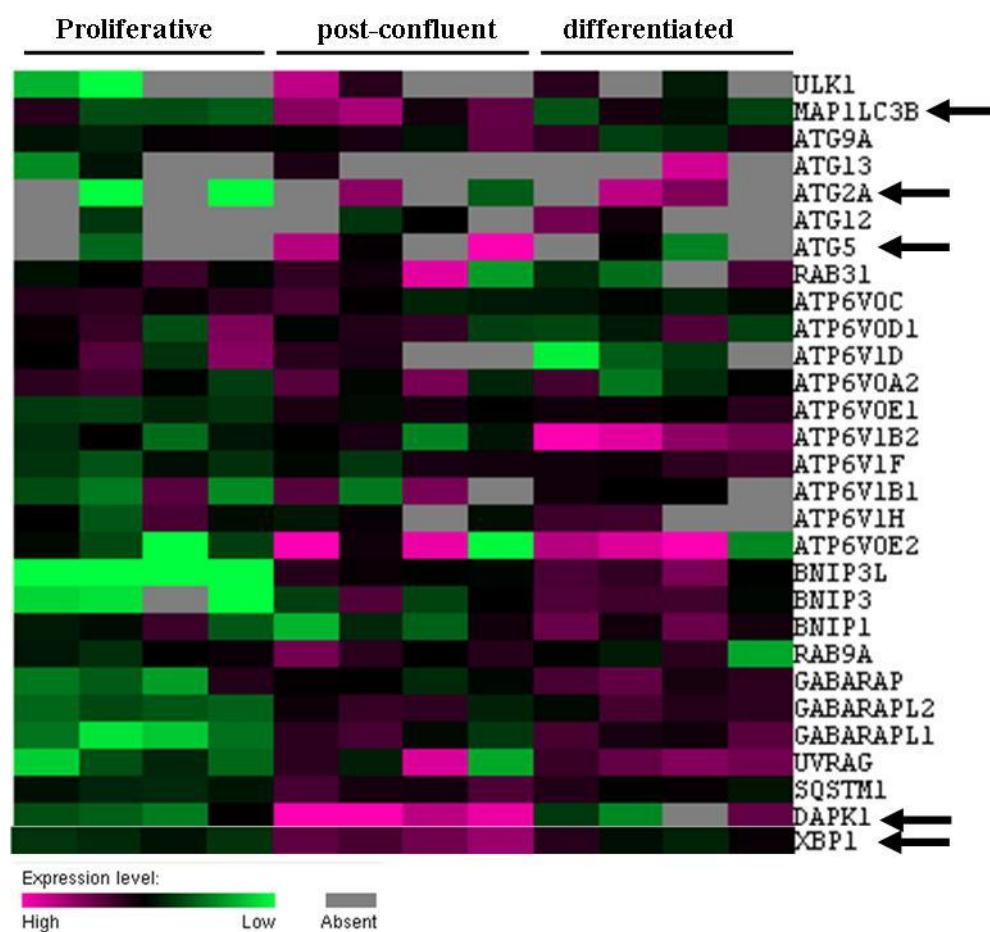
Fig. 3.19 Cluster analyses of possible autophagy related targets of C/EBPβ in differentiating Caco-2 cells from GEO datasets (GDS709). Cluster analyses already available was used to extract autophagy related genes. Pink; upregulated genes, green; downregulated genes, gray; no signal.

A major fraction of all the autophagy related genes involved in the dataset were considered as a target of C/EBPβ in the literature. Among these, a considerable amount was upregulated during differentiation, further confirming the induction of autophagy. Five of the genes that showed a peak in the mid-stages of differentiation are of interest as possible targets for C/EBPβ-3 and may be examined further.

CHAPTER 4

DISCUSSION

In this study, using two colorectal cancer cell lines as established models of cellular differentiation, the pathways regulating differentiation of intestinal epithelial cells were investigated. Intestinal homeostasis is highly dependent on the constant renewal of epithelial cells followed by their differentiation in the crypt – villus axis.

The molecular mechanisms regulating this process are poorly understood and the rapid death of normal (non-transformed) cells isolated from the intestine led to the generation of cellular models of differentiation. Two of these models, Caco-2 and HT-29 colorectal cancer cell lines, have been widely used since their establishment in 1977 (Fogh et al., 1977). Caco-2 cells, grown approximately 20 days after confluency and HT-29 cells grown under glucose deprived conditions 10 days after confluency, exhibited epithelial like morphology with distinct borders, formation of domes and increase in the expression of differentiation markers. The extent of increase in the expression of differentiation markers in HT-29 cells was lower than that of Caco-2 cells in our study, which is consistent with the literature (Simon-Assman et al., 2007).

Extra- and intracellular calcium has been widely reported to regulate cellular growth and differentiation (Cosentino et al., 2010; Ghosh et al., 1991; Short et al., 1993; Whitfield, 2009). Ca^{2+} mobilization from the ER stores was observed during the differentiation of both gastric cancer cells (Papp et al., 2004) and colonic crypts (Lindqvist et al., 1998).We have observed an increase in cytoplasmic Ca^{2+} levels in Caco-2 cells whereas no change was observed in HT-29 cells during the

differentiation process. Ca^{2+} mobilization from the ER stores most likely results from an increase in the levels of the Ca^{2+} pump SERCA3. SERCA3 has less affinity for Ca^{2+} compared to SERCA2 and an increase in SERCA3 results in higher cytoplasmic and diminished ER calcium levels (Lytton et al., 1992). Moreover loss of SERCA3 expression was found to be an early event during colon carcinogenesis (Brouland et al., 2005). Therefore SERCA3 and SERCA2 levels were determined in spontaneously differentiating Caco-2 and HT-29 cells and an increase in SERCA3 was seen only in Caco-2 cells, consistent with the increase in the cytoplasmic Ca^{2+} in these cells. SERCA2 levels did not change in both cell lines.

A key intracellular Ca^{2+} regulator is the ER, providing a site for storage and controlled release of this cation. The increase in the cytoplasmic Ca^{2+} in Caco-2 cells therefore hinted at the presence of ER stress. Examination of the different pathways that lead to ER stress indicated that ER stress was induced in both HT-29 and Caco-2 cells, albeit through different mechanisms.

It is known that glucose deprivation may lead to ER stress; therefore this is most likely the trigger for the induction of ER stress in HT-29 cells. Previously, differential regulation of ER stress in retinoic acid induced differentiation of H9 T lymphocytes and HEK293 cells has been shown (Liu et al., 2012). p-eIF2α and XBP1 were downregulated and BiP was upregulated in H9 cells. On the contrary, HEK293 cells showed a completely different response in which p-eIF2α was induced but BiP and XBP1 were downregulated. It was proposed that while upregulation of certain pathways lead to a stress response, downregulation of the others indicates stress defense. Stress defense is thought to be a protective mechanism from cell death (Liu et al., 2012). Therefore there is no distinct mechanism that is activated or inhibited upon certain stimulation and it can be concluded that the response is always context specific.

Induction of ER stress by SERCA mediated Ca^{2+} release in Caco-2 cells was further confirmed using a SERCA specific inhibitor thapsigargin. Treatment of day 0

(undifferentiated cells with no ER stress) Caco-2 cells with thapsigargin induced p-eIF2α to a similar level as day 10. Moreover when the intracellular/cytoplasmic Ca^{2+} was chelated by BAPTA-AM, a modest inhibition of eIF2α phosphorylation was observed. It was previously shown that in addition to binding Ca^{2+}, BAPTA-AM also inhibits potassium channels independent of Ca^{2+} chelation and therefore may exert other actions in cells (Tang et al., 2007). This may have resulted in the incomplete reversal of the phenotype by BAPTA-AM. eIF2α is the target of four different kinases, PERK, general control non-derepressible (GCN2), protein kinase double stranded RNA dependent (PKR) and heme regulated inhibitor (HRI). However PERK is thought to be the major Ca^{2+} sensor among these kinases (Donnelly et al., 2013). Chemical inhibition of PERK in the differentiating (day 10) Caco-2 cells completely reversed the phosphorylation eIF2α, indicating an active PERK/eIF2α axis in these cells.

In order to survive ER stress, cells frequently initiate signaling pathways that lead to autophagy (Gade et al., 2008; Kouroku et al., 2007; Sakaki and Kaufman, 2008). Autophagy was found to be induced in both HT-29 and Caco-2 cells, however, this induction had a highly temporal nature with ER stress and autophagy peaking at day 10 for Caco-2 cells and day 5 for HT-29 cells, followed by a waning of these responses. It has previously been shown that autophagy levels decreases in differentiated Caco-2 cells (Groulx et al., 2012). However, in this study, the autophagy markers were assayed at the very early (day 5) and very late (day 30) stages of differentiation when the autophagic response had either not been initiated, or was already terminated.

In order to understand if induction of autophagy is downstream of Ca^{2+} induced ER stress, the SERCA pumps were inhibited by thapsigargin in undifferentiated cells and Ca^{2+} flux into the cytoplasm was induced, mimicking mid-stages of differentiation. As expected, autophagy was found to be induced following the induction of eIF2α phosphorylation. ER stress induced autophagy was also confirmed by chelating Ca^{2+} or inhibiting PERK/eIF2α axis leading to the inhibition of autophagy. These results

suggest a role for Ca^{2+} flux from the ER into the cytoplasm in the induction of autophagy. However Ca^{2+} is probably not the only causative factor since chelating it or inhibiting the PERK/eIF2α axis does not rescue the phenotype completely.

To understand whether autophagy was induced in the HT-29 cells, which did not show any Ca^{2+} flux, the autophagy markers were examined. Interestingly, we observed that autophagy; following the induction of ER stress was present in this cell line as well. In the absence of a Ca^{2+} flux, it is likely that autophagy induced through the stress response in HT-29 cells most likely occurs through a different UPR pathway.

The mechanisms leading to ER stress induced autophagy are not well understood. One mechanism that has been proposed was the conversion of LC3I to LC3II by the phosphorylation of PERK/eIF2α (Kouroku et al., 2007). However, the proteins that are activated in between eIF2α phosphorylation and LC3 conversion have not yet been elucidated. The transcription factor C/EBPβ has been implicated in adipocyte, keratinocyte, macrophage differentiation (Lane et al., 1999); Zhu, 1999; Natsuka, 1992} as well as in ER stress (Chen et al., 2004; Li et al., 2008; Meir et al., 2010) and autophagy (Abreu and Sealy, 2010; Gade et al., 2008; Guo et al., 2013). The expression and role of C/EBPβ in the intestinal differentiation is not known. When the protein expression of C/EBPβ was assayed in differentiating Caco-2 and HT-29 cells, it was found to be increased at the mid-stages of the process. C/EBPβ protein exists in three isoforms as a result of alternative translation; C/EBPβ-1, β-2 and β-3. Although C/EBPβ-1 and β-2 levels did not change significantly, the C/EBPβ-3 isoform showed a considerable increase at the mid-stages of differentiation. Interestingly, when the mRNA expression of C/EBPβ was analyzed during cellular differentiation, we observed that the mRNA levels did not change as much as the protein levels, further confirming regulation at the translational level.

The biological effect evoked by C/EBPβ depends highly on the ratio of the isoforms produced in a given cell type. This ratio is controlled through the eukaryotic

initiation factors eIF-2α and eIF-4E (Calkhoven et al., 2000). Full length or short C/EBPβ isoforms arise by differential usage of translation initiation sites, which is mediated by an upstream open reading frame (uORF) conserved through evolution (Calkhoven et al., 2000). It has been proposed that a leaky scanning of ribosomes is responsible for the alternative use of three in-frame methionins, a mechanism observed during ER stress when general translation is inhibited. Other regulatory mechanisms include the phosphorylation and activation of C/EBPβ by PKA and PKC, IL-6 mediated induction during acute phase response through STAT-3 (Ramji and Foka, 2002) and IFNγ mediated induction through MEK-ERK and p38 (Salmenpera et al., 2003). In addition, Ca^{2+}-calmodulin dependent protein kinase II (CaMKII) was also found to phosphorylate C/EBPβ independent of PKC (Wegner et al., 1992).

The increase in C/EBPβ-3 at exactly the same stage as eIF2α and LC3-II suggests a role for this isoform linking the two processes. In accordance with this, the protein levels of C/EBPβ-3 were found to be increased when ER stress was induced in undifferentiated Caco-2 cells by Ca^{2+} flux into the cytoplasm using thapsigargin and the levels were similar to those in day 10 cells. Moreover inhibiting the PERK/eIF2α axis in day 10 differentiating cells completely rescued the phenotype. When we overexpressed C/EBPβ-3 in undifferentiated Caco-2 cells, the p-eIF2α levels did not change (indicating that the phosphorylation of eIF2α occurred upstream of C/EBPβ-3), however, the conversion LC3-I to II was significantly increased. This indicated the effect of C/EBPβ-3 downstream of ER stress and upstream of autophagy thereby implying an important role of this protein in linking these two very important cellular processes.

In HT-29 cells however, a decrease in the phosphorylation of eIF2α was observed during differentiation, which does not correlate with the translational induction of C/EBPβ-3. However, another key regulator of translational initiation in these cells, eIF4E, was found to be inhibited, providing an explanation for the increase in

C/EBPβ-3 levels (Fig. 4.1). There may well be other additional mechanisms for the induction of C/EBPβ in these strictly regulated processes.
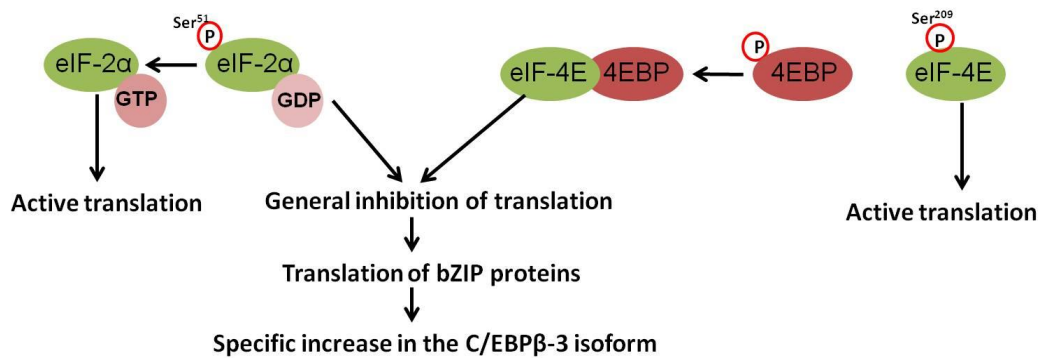
Fig. 4.1 Translational mechanisms leading to increase in C/EBPβ-3. Inhibition of eIF2α via phosphorylation at Ser51 or inhibition of eIF4E via dephosphorylation leads to a general inhibition of translation. This causes a leaky scanning ribosomal machinery and increase in the translation small isoforms of bZIP proteins.

The three axes of the ER stress act in coordination with each other to provide several positive and negative feedbacks (Hetz et al., 2013). For example, the PERK/eIF2/ATF4 axis induces the expression of growth arrest and DNA damage-inducible 34 (GADD34), which in turn participates in a feedback loop to dephosphorylate eIF2α. ATF6 and sXBP1 can act together or individually on their target genes leading to differential expression. uXBP1 was shown to interact with the active form of ATF6 targeting it for proteasomal degradation, which may provide a negative feedback loop to decrease XBP1 expression since one of the targets of ATF6 is XBP1 (Yoshida et al., 2009). In addition, Chen et al. have described increased C/EBPβ expression during UPR, mediated by XBP1 binding to its promoter (Chen et al., 2004). C/EBPβ itself may also be involved in the expression of XBP1 as predicted by Transfac database.

C/EBPβ has been shown to regulate autophagy in a circadian rhythm in the mouse liver (Ma et al., 2011). In breast cancer cells, C/EBPβ-3 was shown to induce autophagy without affecting the cell cycle, apoptosis or necrosis (Abreu and Sealy, 2010). However, the molecular mechanisms of how C/EBPβ induces autophagy have been investigated only in a few studies. The LC3-I cleavage protein Atg4b was shown to be transactivated by C/EBPβ to facilitate adipocyte differentiation (Guo et al., 2013). In mouse liver, C/EBPβ induced autophagy by directly binding to the promoters of Bnip3, Ctsl, and Gabarapl1 (Ma et al., 2011). The role of C/EBPβ in linking ER stress to autophagy has been investigated in a study showing ATF6/ C/EBPβ signaling to induce death associated protein kinase 1 (DAPK1) (Gade et al.). In another study C/EBPβ-3 was induced in late stages of ER stress and led to cell death (Li et al., 2008). However the mechanistic underpinnings linking the specific C/EBPβ-3 isoform to ER stress as well as autophagy has not been reported before. This isoform does not contain a transactivation domain and therefore has widely been thought to have an inhibitory effect on other C/EBPβ isoforms as well as other bZIP family members (Calkhoven et al., 2000). However, very recently, it has been shown that C/EBPβ-3 indeed can bind to the promoter regions of the CXCR4 gene, leading to its transcriptional upregulation in breast cancer cells (Park et al., 2013). When the transcriptional activity of C/EBPβ was investigated in differentiating Caco-2 and HT-29 cells, an increase in the activity was observed for a luciferase plasmid bearing the C/EBPβ consensus site. This finding opposes the inhibitory function of C/EBPβ-3. Additionally, the binding of C/EBPβ to the promoter of sucrase isomaltase, a known target of C/EBPβ, increased on day 10 and then decreased upon completion of differentiation. This pattern again suggests an activating role for C/EBPβ-3. In order to further elucidate the possible autophagy related targets of C/EBPβ, a publicly available microarray dataset was analyzed. Five genes, MAP1LC3B (LC3), Atg2a, Atg5, DAPK1 and XBP1, were identified as potential targets of C/EBPβ and will further be examined. The mechanism of ER stress induced autophagy mediated by C/EBPβ-3 that is proposed in this study is shown in (Fig. 4.2).
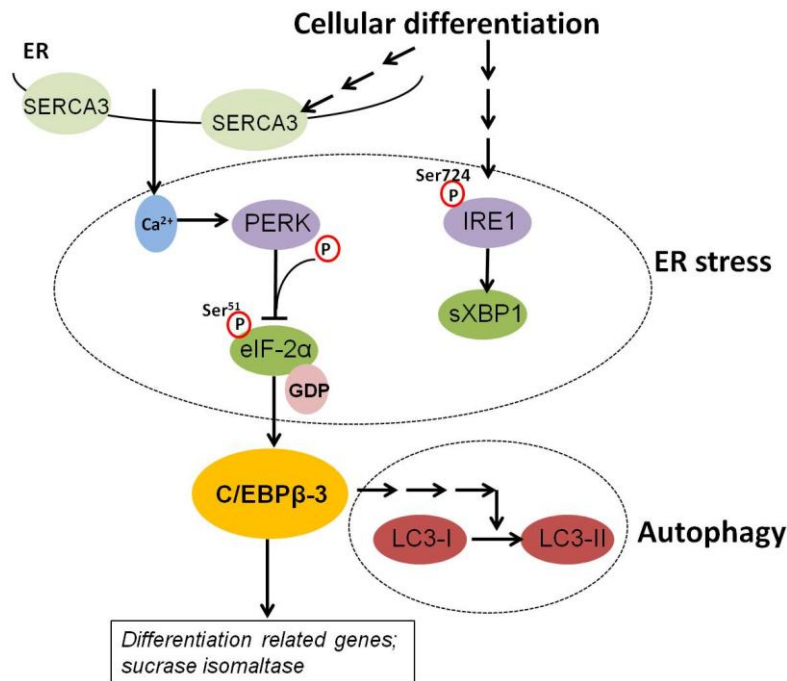
Fig. 4.2 ER stress induced autophagy mediated by C/EBPβ. The differentiation process causes an increase in the SERCA3 levels which has less affinity for calcium, leading to an increase in the cytoplasmic calcium levels. This causes induction of ER stress which in turn activates the autophagy machinery by the help of C/EBPβ-3.

The differentiation of a cell involves global changes in the chromatin structure, transcriptional machinery and thus the whole proteome. Activation of the unfolded protein response is therefore expected and the reason of activation of autophagy during this process may be to compensate the protein load of the ER and provide cell survival. In addition, inflammation caused by ER stress has been shown to be resolved by the activation of autophagy in the intestinal epithelium via inhibition of NF-κB, a key inflammatory transcription factor (Adolph et al., 2013). Accordingly, we have previously shown that NF-κB was inhibited in the differentiationg Caco-2 cells (Astarci et al., 2012). Therefore, another consequence of the induction of autophagy may be to reduce the inflammation caused by ER stress during the differentiation process.

CHAPTER 5

CONCLUSIONS

In this study, the molecular mechanisms regulating intestinal epithelial differentiation were investigated using two well established models of differentiation, Caco-2 and HT-29 colorectal cancer cell lines.

During the differentiation process in Caco-2 and HT-29 cells, ER stress was seen to be induced, which has not been reported previously. In the Caco-2 model, both PERK/eIF2α and IRE1/XBP1 axis of the ER stress response were found to be active. The induction of the stress response resulted from increased cytosolic Ca^{2+} caused by increased expression of SERCA3 pumps with less Ca^{2+} affinity. In the HT-29 model however, only IRE1/XBP1 axis was activated and no Ca^{2+} flux was detected most likely because differentiation was induced in these cells through glucose deprivation.

Induction of autophagy by ER stress was also evidenced in the course of differentiation. This induction was mediated by a key transcription factor C/EBPβ, especially by the short isoform C/EBPβ-3 which is upregulated during ER stress. Although autophagy was shown to be induced by ER stress under certain circumstances, the exact molecular mechanisms were not determined previously. Moreover neither ER stress nor autophagy has been reported to be induced in the intestinal epithelial differentiation models of Caco-2 and HT29 to date.

As a conclusion, ER stress induced autophagy and involvement of C/EBPβ-3 in these processes was for the first time evidenced in the differentiation of Caco-2 and HT-29 cell lines. These results suggest new regulatory mechanisms for the intestinal

epithelial differentiation and provide insights into the investigation of therapeutic targets for colorectal cancer.

REFERENCES

Abreu, M. M., and L. Sealy, 2010, The C/EBPbeta isoform, liver-inhibitory protein (LIP), induces autophagy in breast cancer cell lines: Experimental Cell Research, v. 316, p. 3227-3238.

Adolph, T. E., M. F. Tomczak, L. Niederreiter, H. J. Ko, J. Bock, E. Martinez-Naves, J. N. Glickman, M. Tschurtschenthaler, J. Hartwig, S. Hosomi, M. B. Flak, J. L. Cusick, K. Kohno, T. Iwawaki, S. Billmann-Born, T. Raine, R. Bharti, R. Lucius, M. N. Kweon, S. J. Marciniak, A. Choi, S. J. Hagen, S. Schreiber, P. Rosenstiel, A. Kaser, and R. S. Blumberg, 2013, Paneth cells as a site of origin for intestinal inflammation: Nature, v. 503, p. 272-+.

Amaravadi, R. K., D. N. Yu, J. J. Lum, T. Bui, M. A. Christophorou, G. I. Evan, A. Thomas-Tikhonenko, and C. B. Thompson, 2007, Autophagy inhibition enhances therapy-induced apoptosis in a Myc-induced model of lymphoma: Journal of Clinical Investigation, v. 117, p. 326-336.

Astarci, E., A. Sade, I. Cimen, B. Savas, and S. Banerjee, 2012, The NF-kappa B target genes ICAM-1 and VCAM-1 are differentially regulated during spontaneous differentiation of Caco-2 cells: Febs Journal, v. 279, p. 2966-2986.

Atwood, A. A., and L. Sealy, 2010, Regulation of C/EBPbeta1 by Ras in mammary epithelial cells and the role of C/EBPbeta1 in oncogene-induced senescence: Oncogene, v. 29, p. 6004-6015.

Back, S. H., K. Lee, E. Vink, and R. J. Kaufman, 2006, Cytoplasmic IRE1 alpha-mediated XBP1 mRNA splicing in the absence of nuclear processing and endoplasmic reticulum stress: Journal of Biological Chemistry, v. 281, p. 18691-18706.

Barbara, P. D., G. R. Van den Brink, and D. J. Roberts, 2003, Development and differentiation of the intestinal epithelium: Cellular and Molecular Life Sciences, v. 60, p. 1322-1332.

Behrens, I., and T. Kissel, 2003, Do cell culture conditions influence the carrier-mediated transport of peptides in Caco-2 cell monolayers?: European Journal of Pharmaceutical Sciences, v. 19, p. 433-442.

Bernales, S., K. L. McDonald, and P. Walter, 2006, Autophagy counterbalances endoplasmic reticulum expansion during the unfolded protein response: Plos Biology, v. 4, p. 2311-2324.

Bialik, S., and A. Kimchi, 2006, The death-associated protein kinases: Structure, function, and beyond, Annual Review of Biochemistry: Annual Review of Biochemistry, v. 75: Palo Alto, Annual Reviews, p. 189-210.

Brouland, J. P., P. Gelebart, T. Kovacs, J. Enouf, J. Grossmann, and B. Papp, 2005, The loss of sarco/endoplasmic reticulum calcium transport ATPase 3 expression is an early event during the multistep process of colon carcinogenesis: American Journal of Pathology, v. 167, p. 233-242.

Buck, M., H. Turler, and M. Chojkier, 1994, LAP (NF-IL-6), a tissue-specific transcriptional activator, is an inhibitor of hepatoma-cell proliferation: Embo Journal, v. 13, p. 851-860.

Bundy, L. M., and L. Sealy, 2003, CCAAT/enhancer binding protein beta (C/EBP beta)-2 transforms normal mammary epithelial cells and induces epithelial to mesenchymal transition in culture: Oncogene, v. 22, p. 869-883.

Burgess, A. W., 1998, Growth control mechanisms in normal and transformed intestinal cells: Philosophical Transactions of the Royal Society of London Series B-Biological Sciences, v. 353, p. 903-909.

Calkhoven, C. F., C. Muller, and A. Leutz, 2000, Translational control of C/EBP alpha and C/EBP beta isoform expression: Genes & Development, v. 14, p. 1920-1932.

Chakilam, S., M. Gandesiri, T. T. Rau, A. Agaimy, M. Vijayalakshmi, J. Ivanovska, R. M. Wirtz, J. Schulze-Luehrmann, N. Benderska, N. Wittkopf, A.

Chellappan, P. Ruemmele, M. Vieth, M. Rave-Frank, H. Christiansen, A. Hartmann, C. Neufert, R. Atreya, C. Becker, P. Steinberg, and R. Schneider-Stock, 2013, Death-Associated Protein Kinase Controls STAT3 Activity in Intestinal Epithelial Cells: American Journal of Pathology, v. 182, p. 1005-1020.

Chakraborty, A., N. Bodipati, M. K. Demonacos, R. Peddinti, K. Ghosh, and P. Roy, 2012, Long term induction by pterostilbene results in autophagy and cellular differentiation in MCF-7 cells via ROS dependent pathway: Molecular and Cellular Endocrinology, v. 355, p. 25-40.

Chen, C., E. E. Dudenhausen, Y. X. Pan, C. Zhong, and M. S. Kilberg, 2004, Human CCAAT/enhancer-binding protein beta gene expression is activated by endoplasmic reticulum stress through an unfolded protein response element downstream of the protein coding sequence: Journal of Biological Chemistry, v. 279, p. 27948-27956.

Chinery, R., J. A. Brockman, M. O. Peeler, Y. Shyr, R. D. Beauchamp, and R. J. Coffey, 1997, Antioxidants enhance the cytotoxicity of chemotherapeutic agents in colorectal cancer: A p53-independent induction of p21(WAF1/CIP1) via C/EBP beta: Nature Medicine, v. 3, p. 1233-1241.

Cho, Y. M., Y. S. Jang, Y. M. Jang, S. M. Chung, H. S. Kim, J. H. Lee, S. W. Jeong, I. K. Kim, J. J. Kim, K. S. Kim, and O. J. Kwon, 2009, Induction of unfolded protein response during neuronal induction of rat bone marrow stromal cells and mouse embryonic stem cells: Experimental and Molecular Medicine, v. 41, p. 440-452.

Cosentino, S., C. Gravaghi, E. Donetti, B. M. Donida, G. Lombardi, M. Bedoni, A. Fiorilli, G. Tettamanti, and A. Ferraretto, 2010, Caseinphosphopeptide-induced calcium uptake in human intestinal cell lines HT-29 and Caco2 is correlated to cellular differentiation: Journal of Nutritional Biochemistry, v. 21, p. 247-254.

Degenhardt, K., R. Mathew, B. Beaudoin, K. Bray, D. Anderson, G. H. Chen, C. Mukherjee, Y. F. Shi, C. Gelinas, Y. J. Fan, D. A. Nelson, S. K. Jin, and E.

White, 2006, Autophagy promotes tumor cell survival and restricts necrosis, inflammation, and tumorigenesis: Cancer Cell, v. 10, p. 51-64.

Ding, I. M., Q. D. Wang, Z. H. Dong, and B. M. Evers, 2000, Characterization and regulation of E2F activity during Caco-2 cell differentiation: American Journal of Physiology-Cell Physiology, v. 278, p. C110-C117.

Ding, Q. M., T. C. Ko, and B. M. Evers, 1998, Caco-2 intestinal cell differentiation is associated with G(1) arrest and suppression of CDK2 and CDK4: American Journal of Physiology-Cell Physiology, v. 275, p. C1193-C1200.

Ding, W. X., H. M. Ni, W. T. Gao, Y. F. Hou, M. A. Melan, X. Y. Chen, D. B. Stolz, Z. M. Shao, and X. M. Yin, 2007, Differential effects of endoplasmic reticulum stress-induced autophagy on cell survival: Journal of Biological Chemistry, v. 282, p. 4702-4710.

Donnelly, N., A. M. Gorman, S. Gupta, and A. Samali, 2013, The eIF2 alpha kinases: their structures and functions: Cellular and Molecular Life Sciences, v. 70, p. 3493-3511.

Eaton, E. M., M. Hanlon, L. Bundy, and L. Sealy, 2001, Characterization of C/EBP beta isoforms in normal versus neoplastic mammary epithelial cells: Journal of Cellular Physiology, v. 189, p. 91-105.

Elmore, S. P., T. Qian, S. F. Grissom, and J. J. Lemasters, 2001, The mitochondrial permeability transition initiates autophagy in rat hepatocytes: Faseb Journal, v. 15, p. 2286-+.

Evers, B. M., T. C. Ko, J. Li, and E. A. Thompson, 1996, Cell cycle protein suppression and p21 induction in differentiating Caco-2 cells: American Journal of Physiology-Gastrointestinal and Liver Physiology, v. 271, p. G722-G727.

Fantini, J., B. Abadie, A. Tirard, L. Remy, J. P. Ripert, A. Elbattari, and J. Marvaldi, 1986, Spontaneous and induced dome formation by 2 clonal cell-populations derived from a human adenocarcinoma cell-line, HT29: Journal of Cell Science, v. 83, p. 235-249.

Fogh, J., J. M. Fogh, and T. Orfeo, 1977, 127 Cultured human tumor-cell lines producing tumors in nude mice: Journal of the National Cancer Institute, v. 59, p. 221-226.

Gade, P., G. Ramachandran, U. B. Maachani, M. A. Rizzo, T. Okada, R. Prywes, A. S. Cross, K. Mori, and D. V. Kalvakolanu, 2012, An IFN-gamma-stimulated ATF6-C/EBP-beta-signaling pathway critical for the expression of Death Associated Protein Kinase 1 and induction of autophagy: Proceedings of the National Academy of Sciences of the United States of America, v. 109, p. 10316-10321.

Gade, P., S. K. Roy, H. Li, S. C. Nallar, and D. V. Kalvakolanu, 2008, Critical role for transcription factor C/E.BP-beta in regulating the expression of death-associated protein kinase 1: Molecular and Cellular Biology, v. 28, p. 2528-2548.

Ghosh, T. K., J. Bian, A. D. Short, S. L. Rybak, and D. L. Gill, 1991, Persistent intracellular calcium pool depletion by thapsigargin and its influence on cell-growth: Journal of Biological Chemistry, v. 266, p. 24690-24697.

Gozuacik, D., and A. Kimchi, 2004, Autophagy as a cell death and tumor suppressor mechanism: Oncogene, v. 23, p. 2891-2906.

Groulx, J. F., T. Khalfaoui, Y. D. Benoit, G. Bernatchez, J. C. Carrier, N. Basora, and J. F. Beaulieu, 2012, Autophagy is active in normal colon mucosa: Autophagy, v. 8, p. 893-902.

Grynkiewicz, G., M. Poenie, and R. Y. Tsien, 1985, A new generation of Ca-2+ indicators with greatly improved fluorescence properties: Journal of Biological Chemistry, v. 260, p. 3440-3450.

Guo, L., J. X. Huang, Y. Liu, X. Li, S. R. Zhou, S. W. Qian, H. Zhu, H. Y. Huang, Y. J. Dang, and Q. Q. Tang, 2013, Transactivation of Atg4b by C/EBP beta Promotes Autophagy To Facilitate Adipogenesis: Molecular and Cellular Biology, v. 33, p. 3180-3190.

He, C. C., and D. J. Klionsky, 2009, Regulation Mechanisms and Signaling Pathways of Autophagy: Annual Review of Genetics, v. 43, p. 67-93.

Hetz, C., E. Chevet, and H. P. Harding, 2013, Targeting the unfolded protein response in disease: Nature Reviews Drug Discovery, v. 12, p. 703-719.

Houri, J. J., E. Ogierdenis, D. Destefanis, C. Bauvy, F. M. Baccino, C. Isidoro, and P. Codogno, 1995, Differentiation-dependent autophagy controls the fate of newly synthesized n-linked glycoproteins in the colon adenocarcinoma HT-29 cell-line: Biochemical Journal, v. 309, p. 521-527.

Ilantzis, C., L. Demarte, R. A. Screaton, and C. P. Stanners, 2002, Deregulated expression of the human tumor marker CEA and CEA family member CEACAM6 disrupts tissue architecture and blocks colonocyte differentiation: Neoplasia, v. 4, p. 151-163.

Jang, C. W., C. H. Chen, C. C. Chen, J. Y. Chen, Y. H. Su, and R. H. Chen, 2002, TGF-beta induces apoptosis through Smad-mediated expression of DAP-kinase: Nature Cell Biology, v. 4, p. 51-58.

Johnson, J. P., 1999, Cell adhesion molecules in the development and progression of malignant melanoma: Cancer and Metastasis Reviews, v. 18, p. 345-357.

Kabeya, Y., N. Mizushima, T. Uero, A. Yamamoto, T. Kirisako, T. Noda, E. Kominami, Y. Ohsumi, and T. Yoshimori, 2000, LC3, a mammalian homologue of yeast Apg8p, is localized in autophagosome membranes after processing: Embo Journal, v. 19, p. 5720-5728.

Kaser, A., M. B. Flak, M. F. Tomczak, and R. S. Blumberg, 2011, The unfolded protein response and its role in intestinal homeostasis and inflammation: Experimental Cell Research, v. 317, p. 2772-2779.

Klionsky, D. J., F. C. Abdalla, H. Abeliovich, R. T. Abraham, A. Acevedo-Arozena, K. Adeli, L. Agholme, M. Agnello, P. Agostinis, J. A. Aguirre-Ghiso, H. J. Ahn, O. Ait-Mohamed, S. Ait-Si-Ali, T. Akematsu, S. Akira, H. M. Al-Younes, M. A. Al-Zeer, M. L. Albert, R. L. Albin, J. Alegre-Abarrategui, M. F. Aleo, M. Alirezaei, A. Almasan, M. Almonte-Becerril, A. Amano, R. Amaravadi, S. Amarnath, A. O. Amer, N. Andrieu-Abadie, V. Anantharam, D. K. Ann, S. Anoopkumar-Dukie, H. Aoki, N. Apostolova, G. Arancia, J. P. Aris, K. Asanuma, N. Y. O. Asare, H. Ashida, V. Askanas, D. S. Askew, P.

Auberger, M. Baba, S. K. Backues, E. H. Baehrecke, B. A. Bahr, X. Y. Bai, Y. Bailly, R. Baiocchi, G. Baldini, W. Balduini, A. Ballabio, B. A. Bamber, E. T. W. Bampton, G. Banhegyi, C. R. Bartholomew, D. C. Bassham, R. C. Bast, H. Batoko, B. H. Bay, I. Beau, D. M. Bechet, T. J. Begley, C. Behl, C. Behrends, S. Bekri, B. Bellaire, L. J. Bendall, L. Benetti, L. Berliocchi, H. Bernardi, F. Bernassola, S. Besteiro, I. Bhatia-Kissova, X. N. Bi, M. Biard-Piechaczyk, J. S. Blum, L. H. Boise, P. Bonaldo, D. L. Boone, B. C. Bornhauser, K. R. Bortoluci, I. Bossis, F. Bost, J. P. Bourquin, P. Boya, M. Boyer-Guittaut, P. V. Bozhkov, N. R. Brady, C. Brancolini, A. Brech, J. E. Brenman, A. Brennand, E. H. Bresnick, P. Brest, D. Bridges, M. L. Bristol, P. S. Brookes, E. J. Brown, J. H. Brumell, et al., 2012, Guidelines for the use and interpretation of assays for monitoring autophagy: Autophagy, v. 8, p. 445-544.

Kouroku, Y., E. Fujita, I. Tanida, T. Ueno, A. Isoai, H. Kumagai, S. Ogawa, R. J. Kaufman, E. Kominami, and T. Momoi, 2007, ER stress (PERK/eIF2 alpha phosphorylation) mediates the polyglutamine-induced LC3 conversion, an essential step for autophagy formation: Cell Death and Differentiation, v. 14, p. 230-239.

Kowenz-Leutz, E., and A. Leutz, 1999, A C/EBP beta isoform recruits the SWI/SNF complex to activate myeloid genes: Molecular Cell, v. 4, p. 735-743.

Lacroix, B., M. Kedinger, P. Simonassmann, M. Rousset, A. Zweibaum, and K. Haffen, 1984, Developmental pattern of brush-border enzymes in the human-fetal colon - correlation with some morphogenetic events: Early Human Development, v. 9, p. 95-103.

Lamb, J., S. Ramaswamy, H. L. Ford, B. Contreras, R. V. Martinez, F. S. Kittrell, C. A. Zahnow, N. Patterson, T. R. Golub, and M. E. Ewen, 2003, A mechanism of cyclin D1 action encoded in the patterns of gene expression in human cancer: Cell, v. 114, p. 323-334.

Lane, M. D., Q. Q. Tang, and M. S. Jiang, 1999, Role of the CCAAT enhancer binding proteins (C/EBPs) in adipocyte differentiation: Biochemical and Biophysical Research Communications, v. 266, p. 677-683.

Levine, B., N. Mizushima, and H. W. Virgin, 2011, Autophagy in immunity and inflammation: Nature, v. 469, p. 323-335.

Li, B. X., C. Y. Li, R. Q. Peng, X. J. Wu, H. Y. Wang, D. S. Wan, X. F. Zhu, and X. S. Zhang, 2009, The expression of beclin 1 is associated with favorable prognosis in stage IIIB colon cancers: Autophagy, v. 5, p. 303-306.

Li, Y., E. Bevilacqua, C. B. Chiribau, M. Majumder, C. P. Wang, C. M. Croniger, M. D. Snider, P. F. Johnson, and M. Hatzoglou, 2008, Differential control of the CCAAT/enhancer-binding protein beta (C/EBP beta) products liver-enriched transcriptional activating protein (LAP) and liver- enriched transcriptional inhibitory protein (LIP) and the regulation of gene expression during the response to endoplasmic reticulum stress: Journal of Biological Chemistry, v. 283, p. 22443-22456.

Liang, C., P. Feng, B. Ku, I. Dotan, D. Canaani, B. H. Oh, and J. U. Jung, 2006, Autophagic and tumour suppressor activity of a novel Beclin1-binding protein UVRAG: Nature Cell Biology, v. 8, p. 688-U94.

Liang, X. H., S. Jackson, M. Seaman, K. Brown, B. Kempkes, H. Hibshoosh, and B. Levine, 1999, Induction of autophagy and inhibition of tumorigenesis by beclin 1: Nature, v. 402, p. 672-676.

Lindqvist, S. M., P. Sharp, I. T. Johnson, Y. Satoh, and M. R. Williams, 1998, Acetylcholine-induced calcium signaling along the rat colonic crypt axis: Gastroenterology, v. 115, p. 1131-1143.

Liu, L. H., C. Liu, Y. W. Zhong, A. Apostolou, and S. Y. Fang, 2012, ER stress response during the differentiation of H9 cells induced by retinoic acid: Biochemical and Biophysical Research Communications, v. 417, p. 738-743.

Lytton, J., M. Westlin, S. E. Burk, G. E. Shull, and D. H. Maclennan, 1992, Functional comparisons between isoforms of the sarcoplasmic or

endoplasmic-reticulum family of calcium pumps: Journal of Biological Chemistry, v. 267, p. 14483-14489.

Ma, D., S. Panda, and J. D. D. Lin, 2011, Temporal orchestration of circadian autophagy rhythm by C/EBP beta: Embo Journal, v. 30, p. 4642-4651.

Mahoney, E., D. M. Lucas, S. V. Gupta, A. J. Wagner, S. E. M. Herman, L. L. Smith, Y. Y. Yeh, L. Andritsos, J. A. Jones, J. M. Flynn, K. A. Blum, X. L. Zhang, A. Lehman, H. Kong, M. Gurcan, M. R. Grever, A. J. Johnson, and J. C. Byrd, 2012, ER stress and autophagy: new discoveries in the mechanism of action and drug resistance of the cyclin-dependent kinase inhibitor flavopiridol: Blood, v. 120, p. 1262-1273.

Marciniak, S. J., and D. Ron, 2006, Endoplasmic reticulum stress signaling in disease: Physiological Reviews, v. 86, p. 1133-1149.

Mariadason, J. M., K. L. Rickard, D. H. Barkla, L. H. Augenlicht, and P. R. Gibson, 2000, Divergent phenotypic patterns and commitment to apoptosis of Caco-2 cells during spontaneous and butyrate-induced differentiation: Journal of Cellular Physiology, v. 183, p. 347-354.

Martoriati, A., G. Doumont, M. Alcalay, E. Bellefroid, P. G. Pelicci, and J. C. Marine, 2005, dapk1, encoding an activator of a p19(ARF)-p53-mediated apoptotic checkpoint, is a transcription target of p53: Oncogene, v. 24, p. 1461-1466.

Meir, O., E. Dvash, A. Werman, and M. Rubinstein, 2010, C/EBP-beta Regulates Endoplasmic Reticulum Stress-Triggered Cell Death in Mouse and Human Models: Plos One, v. 5.

Natsuka, S., S. Akira, Y. Nishio, S. Hashimoto, T. Sugita, H. Isshiki, and T. Kishimoto, 1992, Macrophage differentiation-specific expression of NF-IL6, a transcription factor for interleukin-6: Blood, v. 79, p. 460-466.

Nerlov, C., 2007, The C/EBP family of transcription factors: a paradigm for interaction between gene expression and proliferation control: Trends in Cell Biology, v. 17, p. 318-324.

Ogata, M., S. I. Hino, A. Saito, K. Morikawa, S. Kondo, S. Kanemoto, T. Murakami, M. Taniguchi, I. Tanii, K. Yoshinaga, S. Shiosaka, J. A. Hammarback, F. Urano, and K. Imaizumi, 2006, Autophapy is activated for cell survival after endoplasmic reticulum stress: Molecular and Cellular Biology, v. 26, p. 9220-9231.

Papp, B., J. P. Brouland, P. Gelebart, T. Kovacs, and C. Chomienne, 2004, Endoplasmic reticulum calcium. transport ATPase expression during differentiation of colon cancer and leukaemia cells: Biochemical and Biophysical Research Communications, v. 322, p. 1223-1236.

Park, B. H., S. Kook, S. Lee, J. H. Jeong, A. Brufsky, and B. C. Lee, 2013, An isoform of C/EBPbeta, LIP, regulates expression of the chemokine receptor CXCR4 and modulates breast cancer cell migration: J Biol Chem, v. 288, p. 28656-67.

Pfaffl, M. W., 2001, A new mathematical model for relative quantification in real-time RT-PCR: Nucleic Acids Research, v. 29, p. 6.

Pignatelli, M., D. Liu, M. M. Nasim, G. W. H. Stamp, S. Hirano, and M. Takeichi, 1992, MORPHOREGULATORY ACTIVITIES OF E-CADHERIN AND BETA-1 INTEGRINS IN COLORECTAL TUMOR-CELLS: British Journal of Cancer, v. 66, p. 629-634.

Pinto, M., M. D. Appay, P. Simonassmann, G. Chevalier, N. Dracopoli, J. Fogh, and A. Zweibaum, 1982, Enterocytic differentiation of cultured human-colon cancer-cells by replacement of glucose by galactose in the medium: Biology of the Cell, v. 44, p. 193-196.

Pinto, M., S. Robineleon, M. D. Appay, M. Kedinger, N. Triadou, E. Dussaulx, B. Lacroix, P. Simonassmann, K. Haffen, J. Fogh, and A. Zweibaum, 1983, Enterocyte-like differentiation and polarization of the human-colon carcinoma cell-line Caco-2 in culture: Biology of the Cell, v. 47, p. 323-330.

Rabinowitz, J. D., and E. White, 2010, Autophagy and Metabolism: Science, v. 330, p. 1344-1348.

Ramji, D. P., and P. Foka, 2002, CCAAT/enhancer-binding proteins: structure, function and regulation: Biochemical Journal, v. 365, p. 561-575.

Reimold, A. M., N. N. Iwakoshi, J. Manis, P. Vallabhajosyula, E. Szomolanyi-Tsuda, E. M. Gravallese, D. Friend, M. J. Grusby, F. Alt, and L. H. Glimcher, 2001, Plasma cell differentiation requires the transcription factor XBP-1: Nature, v. 412, p. 300-307.

Rousset, M., 1986, the human-colon carcinoma cell-lines HT-29 and Caco-2 - 2 invitro models for the study of intestinal differentiation: Biochimie, v. 68, p. 1035-1040.

Rutkowski, D. T., and R. S. Hegde, 2010, Regulation of basal cellular physiology by the homeostatic unfolded protein response: Journal of Cell Biology, v. 189, p. 783-794.

Sakaki, K., and R. J. Kaufman, 2008, Regulation of ER stress-induced macroautophagy by protein kinase C: Autophagy, v. 4, p. 841-843.

Salmenpera, P., S. Hamalainen, M. Hukkanen, and E. Kankuri, 2003, Interferon-gamma induces C/EBP beta expression and activity through MEK/ERK and p38 in T84 colon epithelial cells: American Journal of Physiology-Cell Physiology, v. 284, p. C1133-C1139.

Sambuy, Y., I. Angelis, G. Ranaldi, M. L. Scarino, A. Stammati, and F. Zucco, 2005, The Caco-2 cell line as a model of the intestinal barrier: influence of cell and culture-related factors on Caco-2 cell functional characteristics: Cell Biology and Toxicology, v. 21, p. 1-26.

Sato, K., K. Tsuchihara, S. Fujii, M. Sugiyama, T. Goya, Y. Atomi, T. Ueno, A. Ochiai, and H. Esumi, 2007, Autophagy is activated in colorectal cancer cells and contributes to the tolerance to nutrient deprivation: Cancer Research, v. 67, p. 9677-9684.

Sebastian, T., R. Malik, S. Thomas, J. Sage, and P. F. Johnson, 2005, C/EBP beta cooperates with RB : E2F to implement Ras(V12)-induced cellular senescence: Embo Journal, v. 24, p. 3301-3312.

Shanmugam, R., P. Gade, A. Wilson-Weekes, H. Sayar, A. Suvannasankha, C. Goswami, L. Li, S. Gupta, A. A. Cardoso, T. Al Baghdadi, K. J. Sargent, L. D. Cripe, D. V. Kalvakolanu, and H. S. Boswell, 2012, A Noncanonical Flt3ITD/NF-kappa B Signaling Pathway Represses DAPK1 in Acute Myeloid Leukemia: Clinical Cancer Research, v. 18, p. 360-369.

Short, A. D., J. H. Bian, T. K. Ghosh, R. T. Waldron, S. L. Rybak, and D. L. Gill, 1993, Intracellular Ca2+ pool content is linked to control of cell-growth: Proceedings of the National Academy of Sciences of the United States of America, v. 90, p. 4986-4990.

Simon-Assman, P., N. Turck, M. Sidhoum-Jenny, G. Gradwohl, and M. Kedinger, 2007, In vitro models of intestinal epithelial cell differentiation: Cell Biology and Toxicology, v. 23, p. 241-256.

Solanas, G., M. Porta-de-la-Riva, C. Agusti, D. Casagolda, F. Sanchez-Aguilera, M. J. Larriba, F. Pons, S. Peiro, M. Escriva, A. Munoz, M. Dunach, A. G. de Herreros, and J. Baulida, 2008, E-cadherin controls beta-catenin and NF-kappa B transcriptional activity in mesenchymal gene expression: Journal of Cell Science, v. 121, p. 2224-2234.

Stappenbeck, T. S., 2010, The role of autophagy in Paneth cell differentiation and secretion: Mucosal Immunology, v. 3, p. 8-10.

Sugiura, K., Y. Muro, K. Futamura, K. Matsumoto, N. Hashimoto, Y. Nishizawa, T. Nagasaka, H. Saito, Y. Tomita, and J. Usukura, 2009, The Unfolded Protein Response Is Activated in Differentiating Epidermal Keratinocytes: Journal of Investigative Dermatology, v. 129, p. 2126-2135.

Sun, L., B. B. Fu, and D. G. Liu, 2005, Systemic delivery of full-length C/EBP beta/liposome complex suppresses growth of human colon cancer in nude mice: Cell Research, v. 15, p. 770-776.

Talloczy, Z., W. X. Jiang, H. W. Virgin, D. A. Leib, D. Scheuner, R. J. Kaufman, E. L. Eskelinen, and B. Levine, 2002, Regulation of starvation- and virus-induced autophagy by the eIF2 alpha kinase signaling pathway: Proceedings

of the National Academy of Sciences of the United States of America, v. 99, p. 190-195.

Tang, Q., M. W. Jin, J. Z. Xiang, M. Q. Dong, H. Y. Sun, C. P. Lau, and G. R. Li, 2007, The membrane permeable calcium chelator BAPTA-AM directly blocks human ether a-go-go-related gene potassium channels stably expressed in HEK 293 cells: Biochemical Pharmacology, v. 74, p. 1596-1607.

Verfaillie, T., M. Salazar, G. Velasco, and P. Agostinis, 2010, Linking ER Stress to Autophagy: Potential Implications for Cancer Therapy: Int J Cell Biol, v. 2010, p. 930509.

Walter, P., and D. Ron, 2011, The Unfolded Protein Response: From Stress Pathway to Homeostatic Regulation: Science, v. 334, p. 1081-1086.

Wang, J. R., 2008, Beclin 1 bridges autophagy, apoptosis and differentiation: Autophagy, v. 4, p. 947-948.

Wegner, M., Z. D. Cao, and M. G. Rosenfeld, 1992, Calcium-regulated phosphorylation within the leucine zipper of C/EBP-beta: Science, v. 256, p. 370-373.

Whitfield, J. F., 2009, The Calcium-Sensing Receptor - A Driver of Colon Cell Differentiation: Current Pharmaceutical Biotechnology, v. 10, p. 311-316.

Wice, B. M., G. Trugnan, M. Pinto, M. Rousset, G. Chevalier, E. Dussaulx, B. Lacroix, and A. Zweibaum, 1985, The intracellular accumulation of UDP-N-acetylhexosamines is concomitant with the inability of human-colon cancer-cells to differentiate: Journal of Biological Chemistry, v. 260, p. 139-146.

Yoshida, H., A. Uemura, and K. Mori, 2009, pXBP1(U), a negative regulator of the unfolded protein response activator pXBP1(S), targets ATF6 but not ATF4 in proteasome-mediated degradation: Cell Struct Funct, v. 34, p. 1-10.

Zalckvar, E., H. Berissi, M. Eisenstein, and A. Kimchi, 2009, Phosphorylation of Beclin 1 by DAP-kinase promotes autophagy by weakening its interactions with Bcl-2 and Bcl-X-L: Autophagy, v. 5, p. 720-722.

Zhang, X. C., E. Szabo, M. Michalak, and M. Opas, 2007, Endoplasmic reticulum stress during the embryonic development of the central nervous system in the mouse: International Journal of Developmental Neuroscience, v. 25, p. 455-463.

Zhu, S. Y., H. S. Oh, M. Shim, E. Sterneck, P. F. Johnson, and R. C. Smart, 1999, C/EBP beta modulates the early events of keratinocyte differentiation involving growth arrest and keratin 1 and keratin 10 expression: Molecular and Cellular Biology, v. 19, p. 7181-7190.

Zweibaum, A., M. Pinto, G. Chevalier, E. Dussauix, N. Triadou, B. Lacroix, K. Haffen, J. L. Brun, and M. Rousset, 1985, Enterocytic differentiation of a subpopulation of the human-colon tumor-cell line HT-29 selected for growth in sugar-free medium and its inhibition by glucose: Journal of Cellular Physiology, v. 122, p. 21-29.

Zweibaum, A., M. Rousset, M. Pinto, G. Chevalier, E. Dussaulx, and J. L. Brun, 1982, Mucus glycoprotein differentiation by serum deprivation of the human-colon carcinoma cell-line HT-29 in culture: Biology of the Cell, v. 45, p. 91-91.

Zwergal, A., M. Quirling, B. Saugel, K. C. Huth, C. Sydlik, V. Poli, D. Neumeier, H. W. L. Ziegler-Heitbrock, and K. Brand, 2006, C/EBP beta blocks p65 phosphorylation and thereby NF-kappa B-mediated transcription in TNF-tolerant cells: Journal of Immunology, v. 177, p. 665-672.

APPENDICES

Appendix A: Cloning C/EBPβ consensus site into pLUC-MCS

C/EBPβ consensus site in three copies (A**TTGCGCAAT**)$_3$ was cloned into HindIII site of pLUC-MCS (Stratagene, CA, USA). Oligos containing three copies of the consensus site and HındIII restriction sites are shown below:

5' - CCC<u>AAGCTT</u>ATTGCGCAATATTGCGCAATATTGCGCAAT<u>AAGCTT</u>GGG – 3'
3' – GGG<u>TTCGAA</u>TAACGCGTTATAACGCGTTATAACGCGTTA<u>TTCGAA</u>CCC – 5'
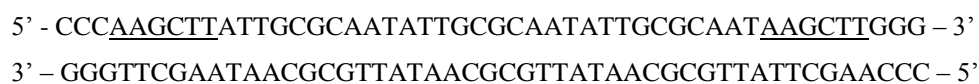
1 µl from the oligo was mixed with 99 ul annealing buffer and heated at 95 °C for 5 min and gradually cooled down to RT. After 95 °C for 5 min, 85°C for 4 min, 80 °C for 4 min, 75°C for 4 min, 70°C for 4 min, 60°C for 4 min, 50°C for 4 min, 37°C for 4 min, 20°C for 4 min, 10°C for 4 min. The recommended reaction conditions for HindIII in Thermo Scientific (Thermo Scientific, <u>http:// www.</u> <u>thermoscientificbio.com/restriction-enzymes/hindiii/</u>, last visited on January 2014) are used. The raction conditions are given in Table A.1

Table A.1 The reaction conditions used for restriction enzyme digestion of insert and pLUC-MCS plasmid.

	Recommended	pLUC-MCS (314,3ng/µl)	Insert (0.1µg/µl)
nuclease-free water	16 µl	13,8	7
10X Buffer R	2 µl	2	2
DNA (1 µg/µl)	1 µl	3,2	10
HindIII	0.5-2 µl (5-10u)	1	1
Total	**20µl**		

Since the same enzyme is used for both termini, the probability of the ends to stick to each other and form an empty vector is high. Therefore the termini are dephosphorylated by alkaline phosphatase and the reannealing is inhibited using FastAP (Fermentas, EF0651) 1u/µl. The reaction conditions are given in Table A.2.

Table A.2 The reaction conditions used for alkaline phosphatase dephosphorylation of linear plasmid DNA.

	Recommended	pLUC-MCS (5.7kb)
nuclease-free water	to 20µl	2
10X Buffer AP	2 µl	2
Linear DNA (~3 kb plasmid)	1µg (~1pmol termini)	15 (0,8µg)
FastAP	µl (1u)	1

The mixture is incubated for 10 min at 37°C and inactivated for 5 min at 75°C. The plasmid is purified by PCR purification kit after dephosphorylation. For the ligation reaction the necessary amounts of plasmid and insert were calculated using Promega biomath calculators (Promega, http://www.promega.com/ techserv/tools/ biomath/calc06.htm, last visited on January 2014). 5:1 insert to vector molar ratio is used for the ligation reaction. The reaction is incubated at 16°C for 16 hours and then the product is directly used for transformation into competent *E. coli*. After the plasmids are isolated, they are sequenced in the central laboratory (Department of Biology, METU).
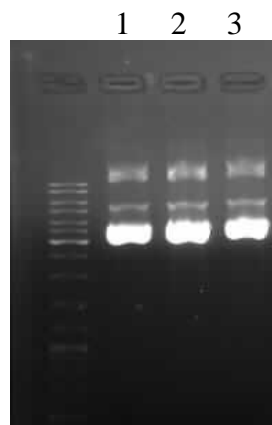
Fig. A.1 The plasmids isolated from colonies 1, 2 and 3.

Appendix B: Competent *E. coli* preparation

1. *E.coli* Top10 was inoculated into 10 ml LB-broth and left at 37˚C with shaking at 240 rpm O/N.

2. Transfer 100 μl of 2,5 ml of culture to each 100 ml LB containing erlen mayer flasks and leave for growing 2-3 h with shaking at 37 ˚C

3. Take OD measurements at 600 nm till desired growth is obtained (*between 0,4-0,6*).

4. Divide E.coli culture into 8 of 50 ml'lik falcons so 25 ml will be included in each.

5. Keep on ice for 10 min and centrifuge at 4ºC at 4000 rpm for 10 min.

6. Resuspend pellet in 5 mL 10 mM CaCl2 by vortexing.

7. Centrifuge at 3000 rpm for 10 min.

8. Re-suspend pellet in each centrifuge tube with 1 ml 75mM CaCl2 *(Prepare prior to compotent preparation).*

9. Add 20% ice cold glycerol (add 200 ml to each 1ml cells).

10. Divide into eppendorf tubes, freeze in liquid nitrogen and store at -80 C.

Appendix C: Transformation of plasmids into competent *E.coli*

1- Thaw competent cells on ice (100µl aliquot)

2- Mix with 50ng plasmid (1µl from 50µl)

3- Incubate on ice for 30 minutes

4- Heat shock at 42°C in water bath for 30 seconds

5- Leave on ice for 2 minutes

6- Add 1 ml LB at 42°C (or 500µl SOC)

7- Shake at 37°C (400 rpm) for 1 hour

8- Plate 200 µl (50µl at least) on LB medium containing the appropriate antibiotic

9- Grow each colony in antibiotic containing LB for maximum 16 hr

10- Isolate plasmids (Qiagen miniprep) and run on 1% agarose gel.

Appendix D : The MIQE Guidelines

Table D.1 *M*inimum *I*nformation for Publication of *Q*uantitative Real-Time PCR *E*xperiments

ITEM TO CHECK	IMPORTANCE	CHECKLIST
EXPERIMENTAL DESIGN		
Definition of experimental and control groups	E	YES
Number within each group	E	YES
Assay carried out by core lab or investigator's lab?	D	YES
Acknowledgement of authors' contributions	D	NO
NUCLEIC ACID EXTRACTION		
Procedure and/or instrumentation	E	YES
Name of kit and details of any modifications	E	YES
Source of additional reagents used	D	YES
Details of DNase or RNAse treatment	E	YES
Contamination assessment (DNA or RNA)	E	NO
Nucleic acid quantification	E	YES
Instrument and method	E	YES
Purity (A260/A280)	D	YES
Yield	D	YES
RNA integrity method/instrument	E	YES
RIN/RQI or Cq of 3' and 5' transcripts	E	NO
Electrophoresis traces	D	N/A
Inhibition testing (Cq dilutions, spike or other)	E	YES
REVERSE TRANSCRIPTION		
Complete reaction conditions	E	YES
Amount of RNA and reaction volume	E	YES
Priming oligonucleotide and concentration	E	YES
Reverse transcriptase and concentration	E	YES
Temperature and time	E	YES
Manufacturer of reagents and catalogue numbers	D	YES
Cqs with and without RT	D	NO
Storage conditions of cDNA	D	YES
qPCR TARGET INFORMATION		
If multiplex, efficiency and LOD of each assay.	E	N/A
Sequence accession number	E	YES
Location of amplicon	D	NO
Amplicon length	E	YES
In silico specificity screen (BLAST, etc)	E	YES
Pseudogenes, retropseudogenes or other homologs?	D	NO
Sequence alignment	D	NO
Secondary structure analysis of amplicon	D	NO
Location of each primer by exon or intron (if applicable)	E	YES
What splice variants are targeted?	E	N/A

Table D.1 continued

qPCR OLIGONUCLEOTIDES

Primer sequences	**E**	**YES**
RTPrimerDB Identification Number	D	**N/A**
Probe sequences	D	**N/A**
Location and identity of any modifications	**E**	**N/A**
Manufacturer of oligonucleotides	D	**YES**
Purification method	D	**NO**

qPCR PROTOCOL

Complete reaction conditions	**E**	**YES**
Reaction volume and amount of cDNA/DNA	**E**	**YES**
Primer, (probe), Mg++ and dNTP concentrations	**E**	**YES**
Polymerase identity and concentration	**E**	**YES**
Buffer/kit identity and manufacturer	**E**	**YES**
Exact chemical constitution of the buffer	D	**N/A**
Additives (SYBR Green I, DMSO, etc.)	**E**	**YES**
Manufacturer of plates/tubes and catalog number	D	**YES**
Complete thermocycling parameters	**E**	**YES**
Reaction setup (manual/robotic)	D	**NO**
Manufacturer of qPCR instrument	**E**	**YES**

qPCR VALIDATION

Evidence of optimization (from gradients)	D	YES
Specificity (gel, sequence, melt, or digest)	**E**	**YES**
For SYBR Green I, Cq of the NTC	**E**	**YES**
Standard curves with slope and y-intercept	**E**	**YES**
PCR efficiency calculated from slope	**E**	**YES**
Confidence interval for PCR efficiency or standard error	D	**N/A**
r2 of standard curve	**E**	**YES**
Linear dynamic range	**E**	**YES**
Cq variation at lower limit	**E**	**YES**
Confidence intervals throughout range	D	**N/A**
Evidence for limit of detection	**E**	**YES**
If multiplex, efficiency and LOD of each assay.	**E**	**N/A**

DATA ANALYSIS

qPCR analysis program (source, version)	**E**	**YES**
Cq method determination	**E**	**YES**
Outlier identification and disposition	**E**	**N/A**
Results of NTCs	**E**	**YES**
Justification of number and choice of reference genes	**E**	**YES**
Description of normalization method	**E**	**YES**
Number and concordance of biological replicates	D	**YES**
Number and stage (RT or qPCR) of technical replicates	**E**	**YES**
Repeatability (intra-assay variation)	E	**YES**
Reproducibility (inter-assay variation, %CV)	D	**NO**
Power analysis	D	**NO**
Statistical methods for result significance	**E**	**YES**
Software (source, version)	**E**	**YES**
Cq or raw data submission using RDML	D	N/A

E: Essential information, D: Desirable information, N/A: Not applicable
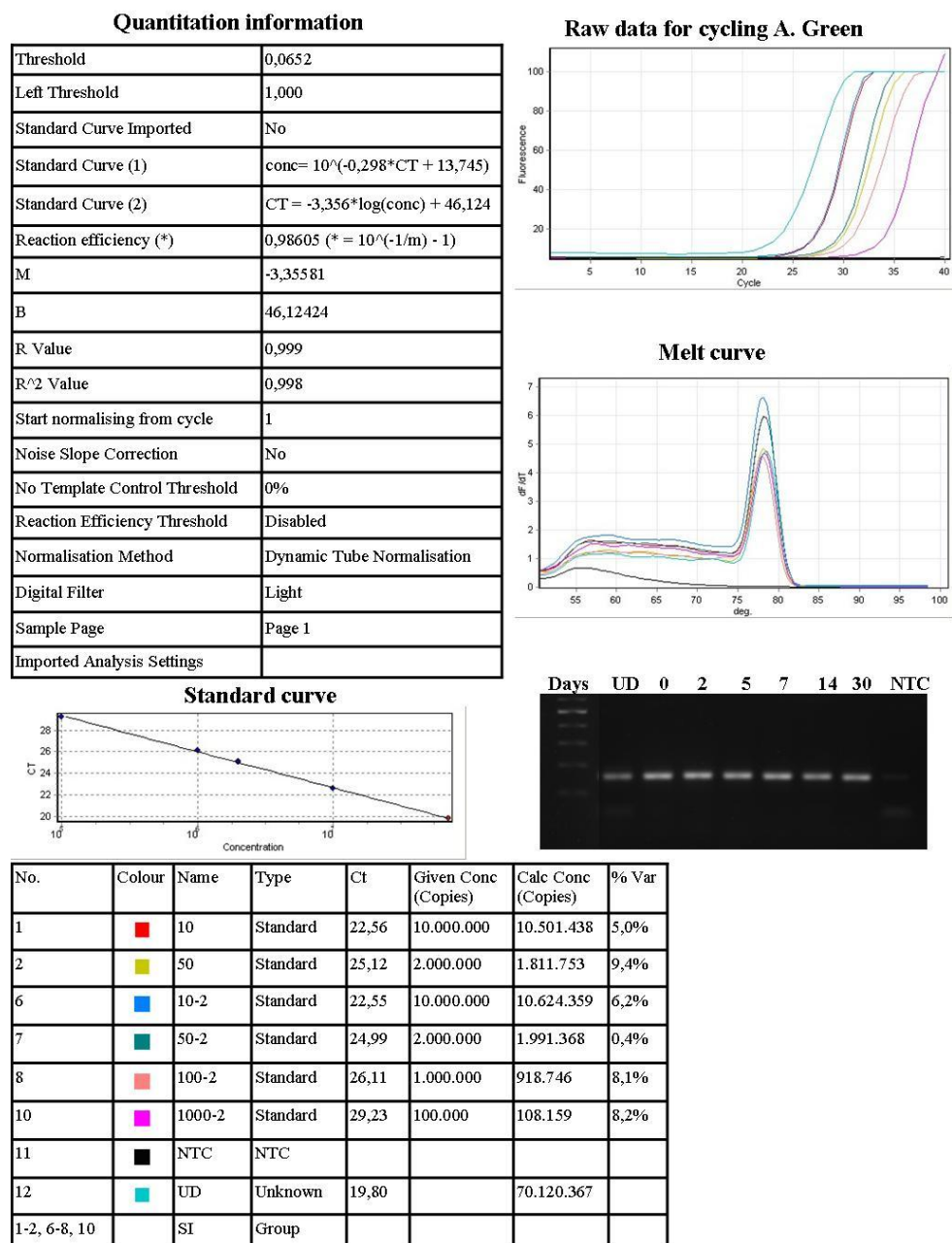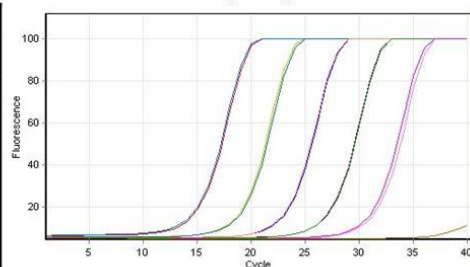
Appendix E: Standard curves

Quantitation information

Threshold	0,0652
Left Threshold	1,000
Standard Curve Imported	No
Standard Curve (1)	conc= $10^{\wedge}(-0,298*CT + 13,745)$
Standard Curve (2)	CT = -3,356*log(conc) + 46,124
Reaction efficiency (*)	0,98605 (* = $10^{\wedge}(-1/m) - 1$)
M	-3,35581
B	46,12424
R Value	0,999
R^2 Value	0,998
Start normalising from cycle	1
Noise Slope Correction	No
No Template Control Threshold	0%
Reaction Efficiency Threshold	Disabled
Normalisation Method	Dynamic Tube Normalisation
Digital Filter	Light
Sample Page	Page 1
Imported Analysis Settings	

Raw data for cycling A. Green

Melt curve

Standard curve

No.	Colour	Name	Type	Ct	Given Conc (Copies)	Calc Conc (Copies)	% Var
1	(red)	10	Standard	22,56	10.000.000	10.501.438	5,0%
2	(yellow)	50	Standard	25,12	2.000.000	1.811.753	9,4%
6	(blue)	10-2	Standard	22,55	10.000.000	10.624.359	6,2%
7	(teal)	50-2	Standard	24,99	2.000.000	1.991.368	0,4%
8	(pink)	100-2	Standard	26,11	1.000.000	918.746	8,1%
10	(magenta)	1000-2	Standard	29,23	100.000	108.159	8,2%
11	(black)	NTC	NTC				
12	(cyan)	UD	Unknown	19,80		70.120.367	
1-2, 6-8, 10		SI	Group				

Fig. E.1 Standard curve and confirmation of the reaction on agarose gel for sucrase isomaltase.

Quantitation information

Threshold	0.1957
Left Threshold	1.000
Standard Curve Imported	No
Standard Curve (1)	conc= 10^(-0.250*CT + 11.074)
Standard Curve (2)	CT = -3.997*log(conc) + 44.259
Reaction efficiency (*)	0.77915 (* = 10^(-1/m) - 1)
M	-3.9966
B	44.25927
R Value	0.99993
R^2 Value	0.99987
Start normalising from cycle	1
Noise Slope Correction	No
No Template Control Threshold	0%
Reaction Efficiency Threshold	Disabled
Normalisation Method	Dynamic Tube Normalisation
Digital Filter	Light
Sample Page	Page 1
Imported Analysis Settings	

Raw data for cycling A. Green

Melt curve

Standard curve

No.	Colour	Name	Type	Ct	Given Conc (copies/ul)	Calc Conc (copies/ul)	% Var
1	■	Undil 1	Standard	12.31	100,000,000	98,728,449	1.3%
2	■	10X 1	Standard	16.29	10,000,000	9,959,283	0.4%
3	■	100x 1	Standard	20.26	1,000,000	1,013,991	1.4%
4	■	1000X 1	Standard	24.25	100,000	101,597	1.6%
5	■	10000X 1	Standard	28.44	10,000	9,106	8.9%
6	■	Undil 2	Standard	12.27	100,000,000	100,780,452	0.8%
7	■	10X 2	Standard	16.31	10,000,000	9,857,371	1.4%
8	■	100x 2	Standard	20.27	1,000,000	1,005,940	0.6%
9	■	1000X 2	Standard	24.24	100,000	102,015	2.0%
10	■	10000X 2	Standard	28.17	10,000	10,634	6.3%
11	■	NTC	NTC	38.68		25	
1-11		GAPDH	Group				

Fig. E.2 Standard curve and confirmation of the reaction on agarose gel for GAPDH.

Quantitation information

|	
Threshold	0,0604
Left Threshold	1,000
Standard Curve Imported	No
Standard Curve (1)	conc= 10^(-0,285*CT + 11,079)
Standard Curve (2)	CT = -3,504*log(conc) + 38,823
Reaction efficiency (*)	0,92922 (* = 10^(-1/m) - 1)
M	-3,50408
B	38,82271
R Value	0,9978
R^2 Value	0,99561
Start normalising from cycle	11
Noise Slope Correction	Yes
No Template Control Threshold	0%
Reaction Efficiency Threshold	Disabled
Normalisation Method	Dynamic Tube Normalisation
Digital Filter	Light
Sample Page	Page 1
Imported Analysis Settings	

Quantitation data for cycling A. Green
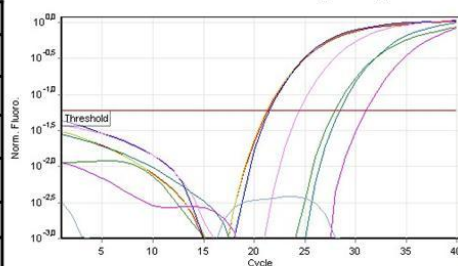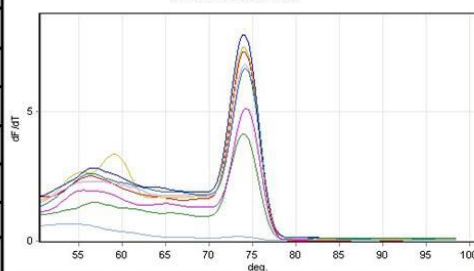
Melt curve
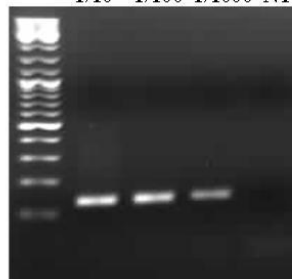
Standard curve
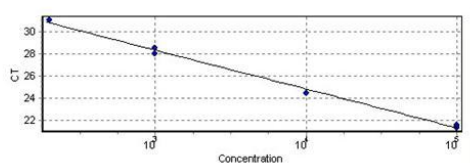
No.	Colour	Name	Type	Ct	Given Conc (Copies)	Calc Conc (Copies)	% Var
33		10-1	Standard	21,40	100.000	93.814	6,2%
34		10-2	Standard	21,27	100.000	101.893	1,9%
35		10-3	Standard	21,52	100.000	86.503	13,5%
37		100-2	Standard	24,42	10.000	12.907	29,1%
39		1000-1	Standard	28,47	1.000	898	10,2%
41		1000-3	Standard	27,97	1.000	1.247	24,7%
42		5000-1	Standard	31,03	200	167	16,4%
48		NTC	NTC				
33-35, 37, 39, 41-42, 48		3	Group				

Fig. E.3 Standard curve and confirmation of the reaction on agarose gel for sucrase isomaltase ChIP primers.

The pLuc-MCS Plasmid
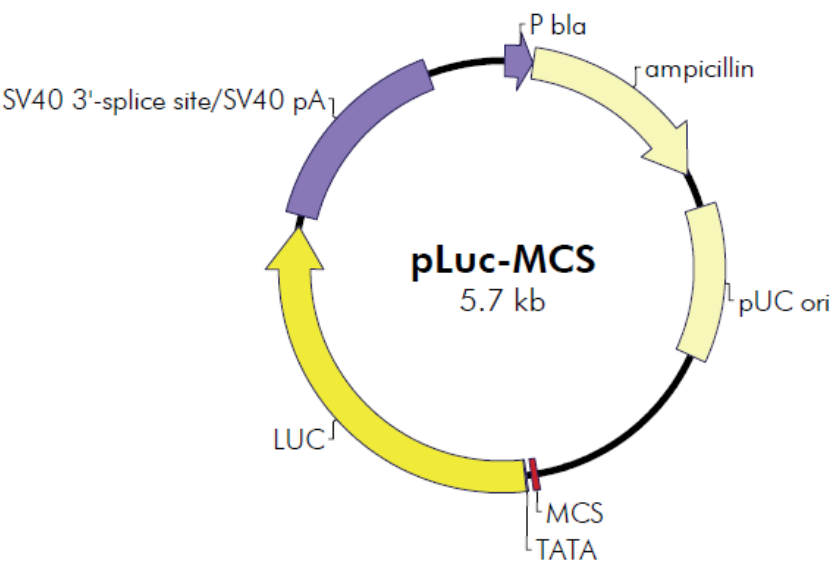
pLuc-MCS Multiple Cloning Site Region
(sequence shown 2682–2737)

```
Hind III  Srf I  Sma I/Xma I  Bgl II      Xho I       Sal I                                    TATA box
  |          |      | |          |           |           |                                        |
AAGCTTGCCCGGGCAGATCTCTCGAGGTCGACAGCGGAGACTCTAGAGGGTATATA
```
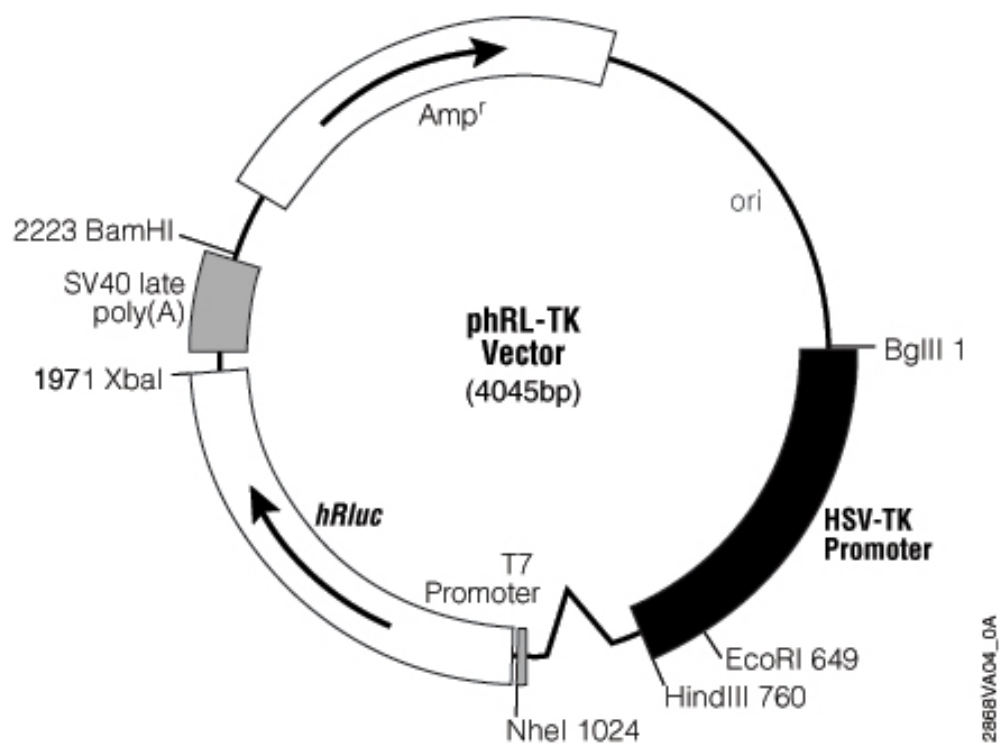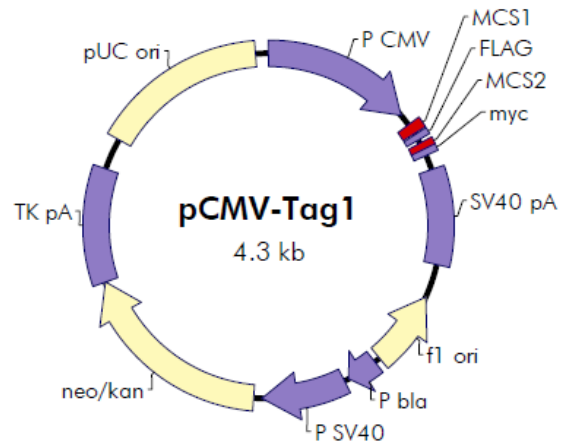
Fig. F.1 pLUC-MCS (Stratagene).

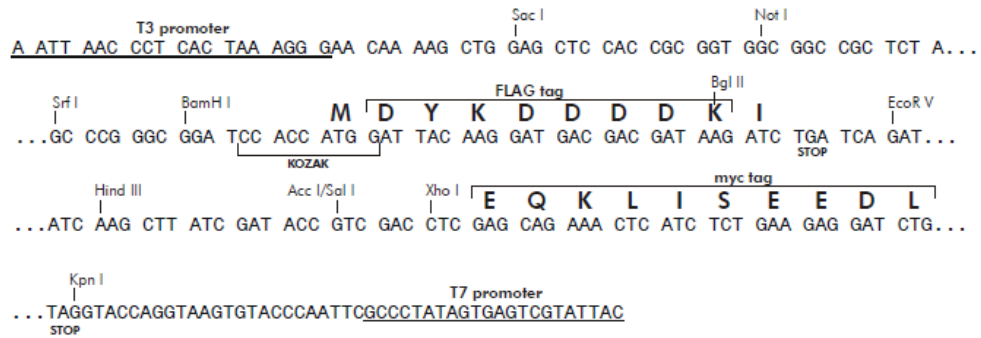Fig. F.2 phRL-TK vector (Promega)

Fig. F.3 pCMV-Tag1 vector (Stratagene)

Apendix G: Buffers for Western Blot

10 X Blotting buffer (1 L)

30.3 g Trizma Base (0.25M)

144 g Glycine (1.92 M)

pH ˜ 8.3

Transfer Buffer (2L)

400 ml Methanol

200 ml 10 X Blotting buffer

1400 ml water

Mild Stripping Buffer

15g glycine

1 g SDS

10 ml Tween 20

Adjust the pH to 2,2

Complete to 1L with distilled water

Harsh Stripping Buffer

100 mM β-meOH

2% SDS,

62.5 mM Tris-HCl pH: 6.8

6X Sample Loading Buffer

12% SDS

30% Beta-mercaptaethanol

30% Glycerol

0.012% Bromophenol blue

0.375M Tris HCl pH:6.8

TBS-T

50mM Tris-HCl H:7.4

150mM NaCl

0.1% Tween 20

12% Seperating Gel Mix

3.8 ml 10%SDS+1.5M TrisHCl pH 8.8

6.7ml of Acrylamide (30%T)

150 μl APS

20 μl TEMED

4.3 ml dH2O

4% Stacking Gel Mix

2 ml 10%SDS+1.5M TrisHCl pH 6.8

1.2 ml of Acrylamide (30%T)

50 μl APS

10 μl TEMED

4.7 ml dH2O

SDS-PAGE Buffer

25 mM Tris base

190 mM glycine

0.1% SDS

PBS-T Washing Buffer

8 g NaCl

0.27 g KH2PO4

3.58 g Na2HPO4 12 H2O

Adjust pH to 7.4 with HCl and autoclave

Add 0.1% Tween 20 prior to use

CURRICULUM VITAE

PERSONAL INFORMATION

Surname, Name: Sade Memişoğlı, Aslı

Nationality: Turkish citizen

Date and Place of Birth: 11th May 1980, Ankara/TURKEY

Marital Status: Married

Phone: +90 (542) 374 04 64

Email: asli.sade@gmail.com

EDUCATION

Degree	Institution	Year of Graduation
MSc	METU Biology	2009
BSc	METU Biology	2002
High School	TED Ankara College Foundation	1997

WORK EXPERIENCE

Year	Place	Enrollment
2005 – 2006	Aktüel Tıp Dergisi (Journal of Current Medicine)	Advertising Coordinator and Medical Translator
2004 – 2005	Eczacıbaşı Pharmaceuticals	Medical Sales Representative
2001	Düzen Laboratories	Summer Practice, Microbiology – Biotechnology

FOREIGN LANGUAGES

Advanced English

PUBLICATIONS

SCI PAPERS

Astarci E, **Sade A**, Çimen I, Savaş B and Banerjee S. The NF-κB target genes ICAM-1 and VCAM-1 are differentially regulated during spontaneous differentiation of Caco-2 cells. FEBS J. 2012, 279, 2966-86.

Sade A, Tunçay S, Çimen I, Severcan F, Banerjee S . Celecoxib reduces fluidity and decreases metastatic potential of colon cancer cell lines irrespective of COX-2 expression. Bioscience Reports 2012, 32, 35-44.

Sade A, Banerjee S, Severcan F**.** Effects of the non steroidal anti-inflammatory drug celecoxib on cholesterol containing distearoyl phosphatidylcholine membranes. Spectroscopy - An international journal. 2011, 25, 177-185.

Deniz A, **Sade A**, Severcan F, TezcanerA, Keskin D, Banerjee S . Celecoxib Loaded Liposomes: Effect of Cholesterol on Encapsulation and *in vitro* Release Characteristics.Biosci Rep. 2010 Jun 3;30(5):365-73.

Sade A, Banerjee S and Severcan F. Concentration dependent effects of celecoxib on model membranes. J Liposome Res. 2010 Jun;20(2):168-77.

ISI CURRENT WEB CONTENTS PAPERS:

Sade A, **Banerjee S** . SPAM1 (sperm adhesion molecule 1 (PH-20 hyaluronidase, zona pellucida binding)). Atlas Genet Cytogenet Oncol Haematol. March 2010 . URL: http://AtlasGeneticsOncology.org/Genes/SPAM1ID42361ch7q31.html

MEETINGS AND SEMINARS

Sade Memisoglu A, Banerjee S. Regulation and role of CCAAT/enhancer binding protein during differentiation of intestinal epithelial cells, The European Cancer Congress, September 27-October 2, 2013, Amsterdam, Holland.

Sade A, Tunçay S, Çimen İ, Severcan F ve Banerjee S. Biophysical and functional characterization of celecoxib in colorectal cancer cell lines. 4th International Meeting on Medicinal and Pharmaceutical Chemistry & 6th International Symposium on Pharmaceutical Chemistry, 30 Eylül – 2 Ekim, 2010 Ankara, Türkiye.

Sade A, Banerjee S and Severcan F. Concentration dependent effects of celecoxib on model membranes. 9th International Symposium on Pharmaceutical Sciences, June 23-26, 2009, Ankara, Turkey.

Sade A, Erdoğ A, Severcan F ve Banerjee S. Selekoksib ile DSPC lipozomların etkileşiminin FTIR spektroskopisi ile incelenmesi. BİYOMUT 08, 29-31 Mayıs 2008, ODTÜ.

Sade A, Severcan F and Banerjee S. Plasmid DNA transfection in the colorectal cancer cell line HCT-116 significantly alters cellular characteristics. EMBO Young Scientists Forum Boğaziçi University 20-22 Feb 2008.

HOBBIES

Rhythmic gymnastics, reading, contemporary dance.